



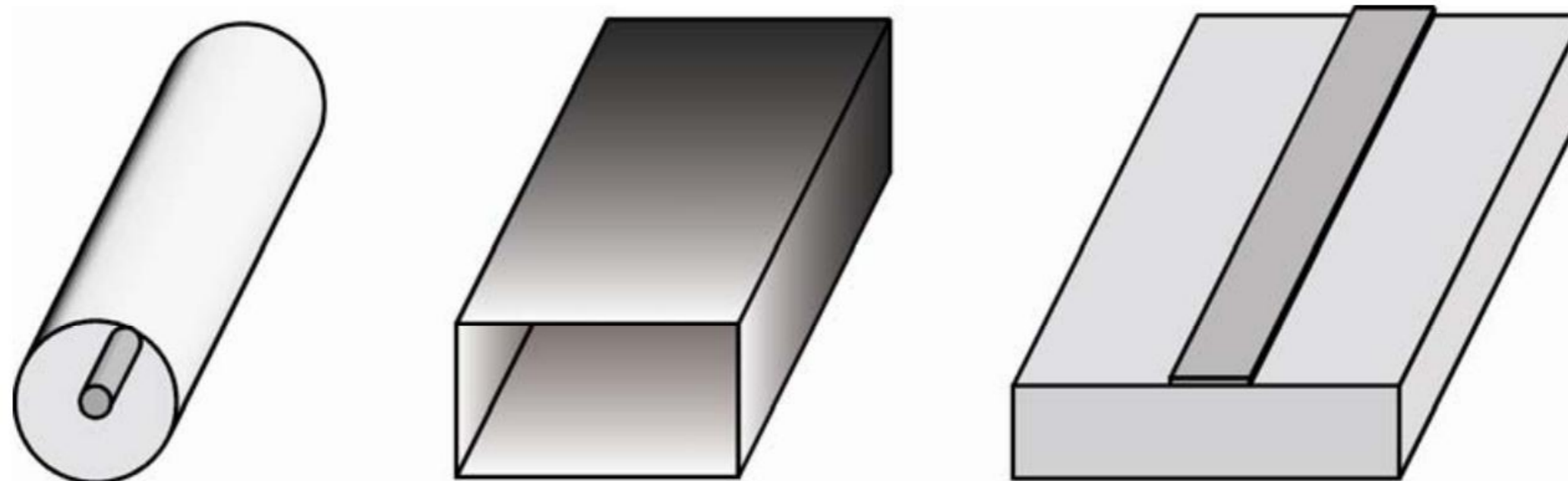
Microstrip Antennas

Antennas

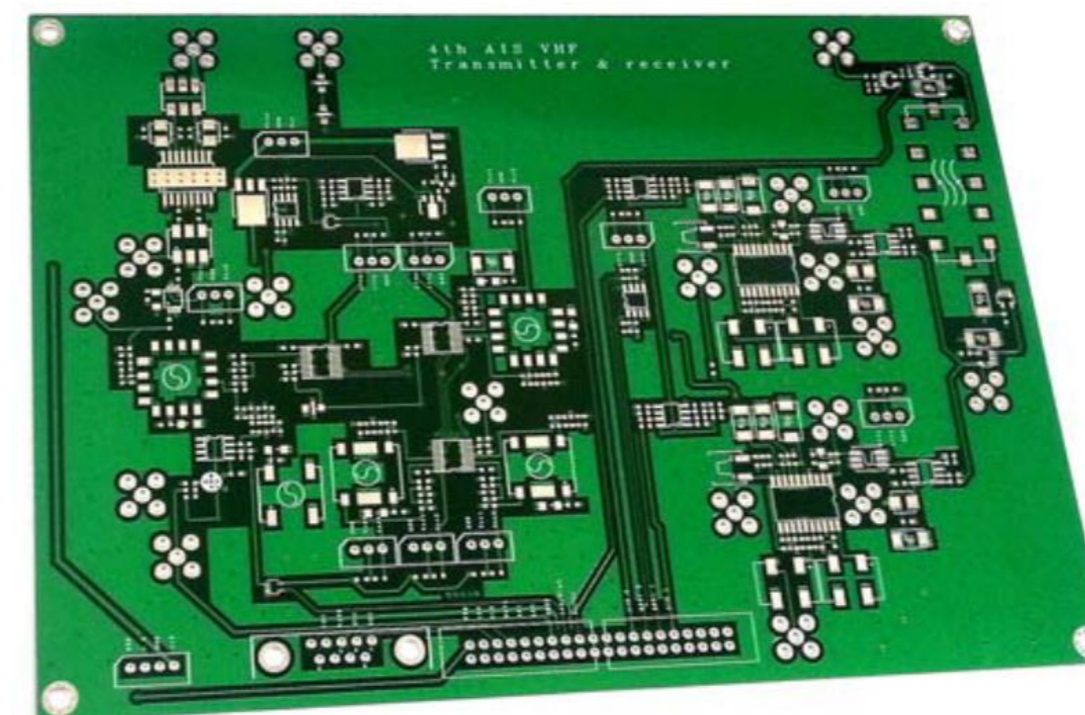
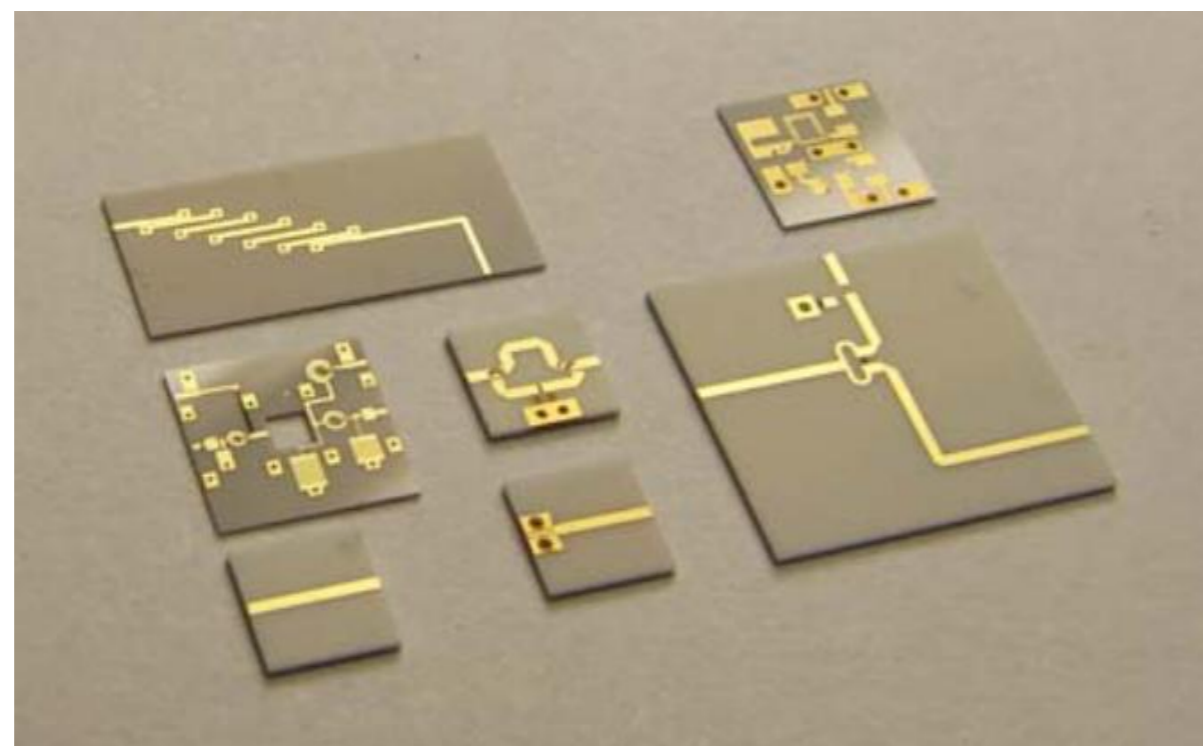
Amir Jafargholi, STI-LWE
amir.jafargholi@epfl.ch

- What is microstrip antenna
- Feeding methods
- Transmission line analysis
- Cavity method analysis
- Antenna performance
- Mutual coupling and array
- Circular polarization

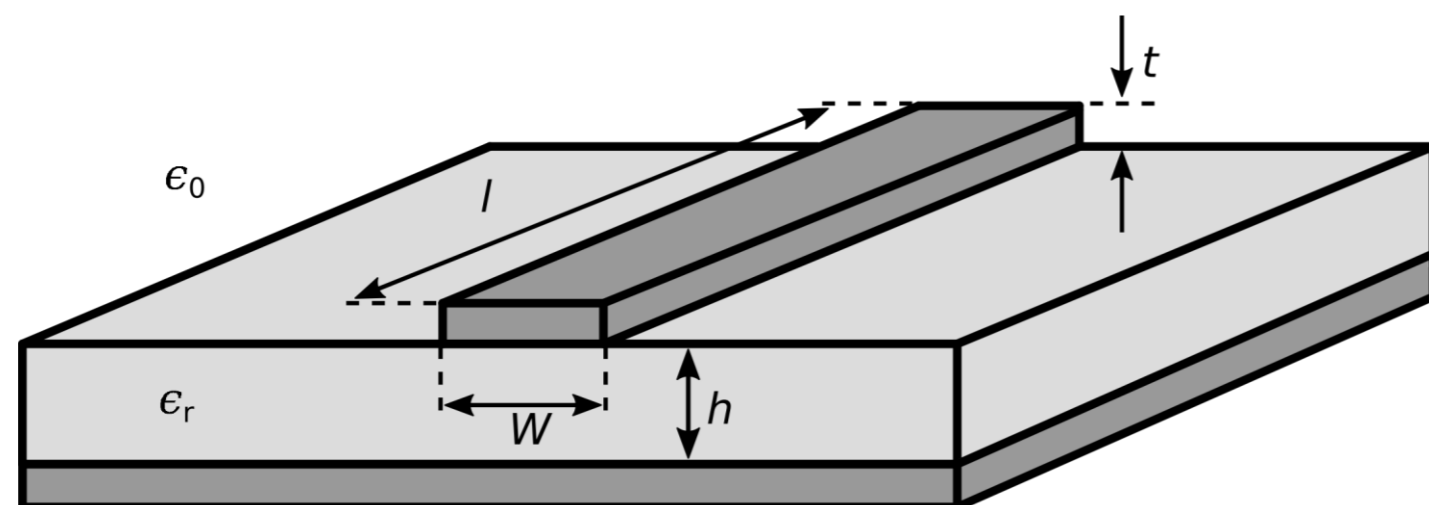
What is the Microstrip?



(i) coaxial line (ii) rectangular waveguide, and (iii) microstrip line



What is the Microstrip?

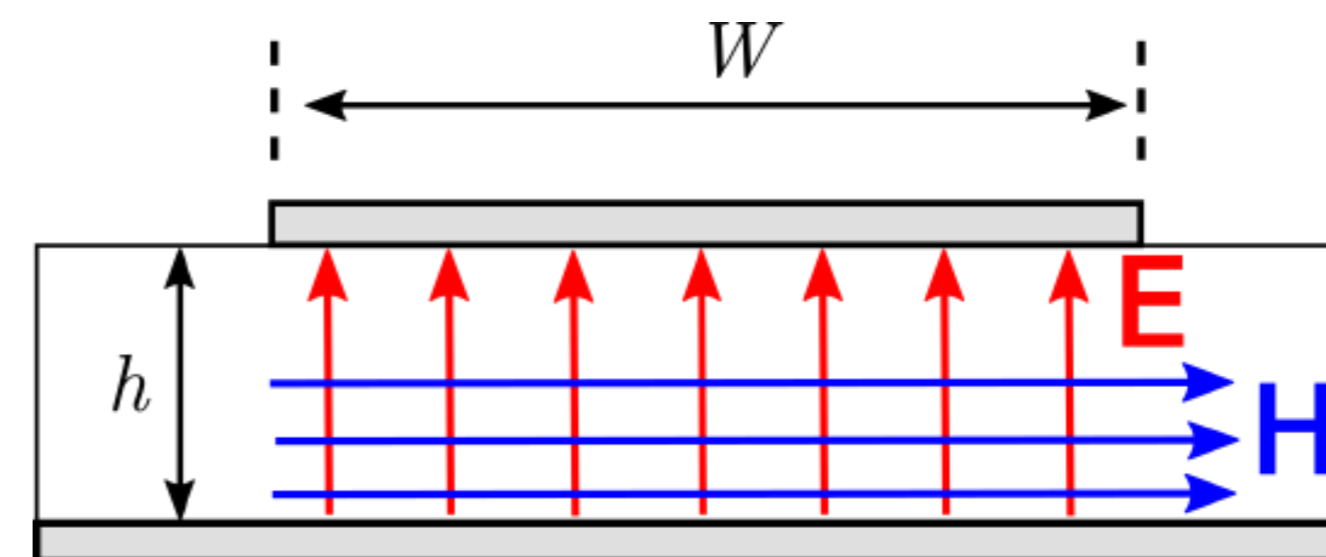


Microstrip transmission line structure and design parameters

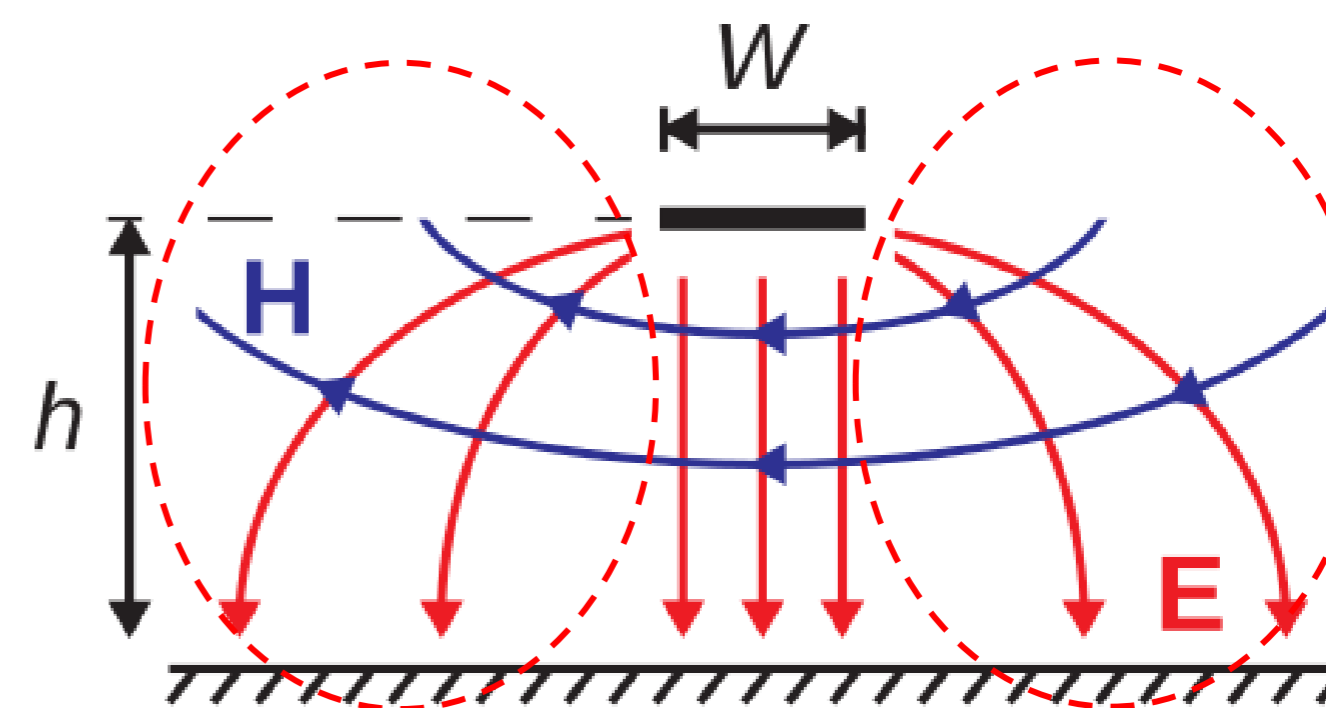
As can be seen, most of the electric field lines reside in the substrate and parts of some lines exist in air. As $W/h \gg 1$ and $\epsilon_r \gg 1$, the electric field lines concentrate mostly in the substrate. Fringing in this case makes the microstrip line look wider electrically compared to its physical dimensions. Since some of the waves travel in the substrate and some in air, an effective dielectric constant ϵ_{reff} is introduced to account for fringing and the wave propagation in the line. For a line with air above the substrate, the effective dielectric constant has values in the range of $1 < \epsilon_{reff} < \epsilon_r$. For most applications where the dielectric constant of the substrate is much greater than unity ($\epsilon_r \gg 1$), the value of ϵ_{reff} will be closer to the value of the actual dielectric constant ϵ_r of the substrate.

$$\frac{W}{h} > 1$$

$$\epsilon_{reff} = \frac{\epsilon_r + 1}{2} + \frac{\epsilon_r - 1}{2} \left[1 + 12 \frac{h}{W} \right]^{-1/2}$$



Approximate structure of the electric and magnetic fields within microstrip line



Electric and magnetic fields lines for narrow ($W \ll h$)

Microstrip Antenna

- One of the most useful antennas at microwave frequencies ($f > 1$ GHz).
- It usually consists of a metal “patch” on top of a grounded dielectric substrate.
- The patch may be in a variety of shapes, but rectangular and circular are the most common:

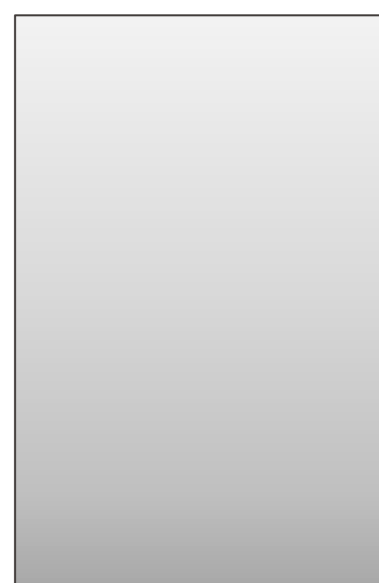


Georges A. Deschamps
1911-1998



Robert E. Munson
1940-2015

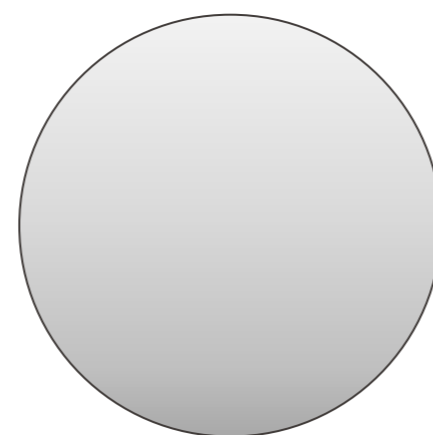
Antennas



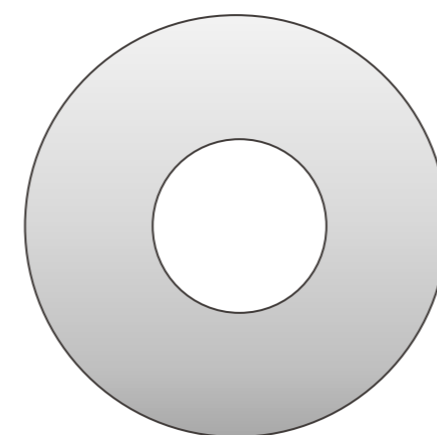
Rectangular



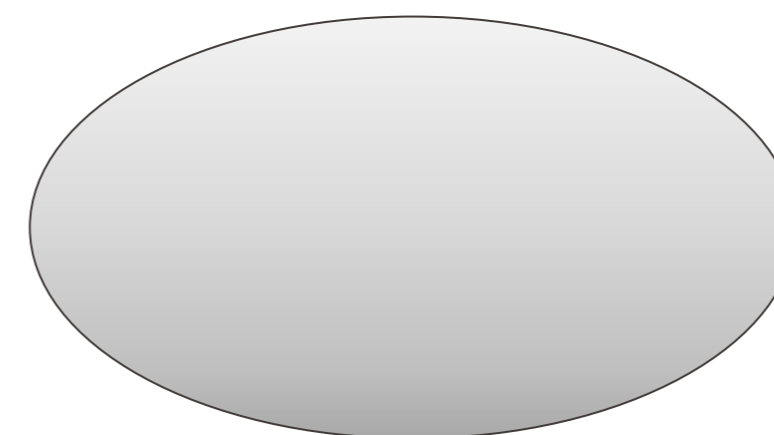
Square



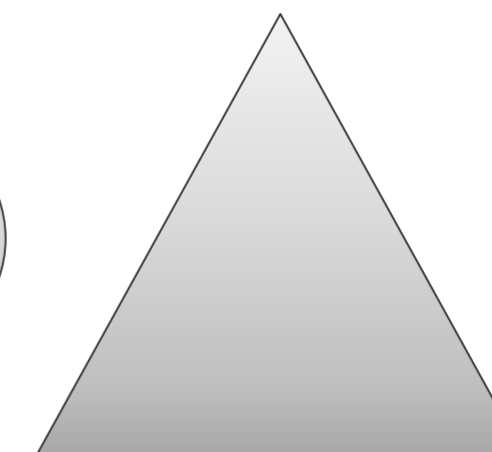
Circular



Annular ring



Elliptical



Triangular

G. A. Deschamps, “Microstrip Microwave Antennas,” Presented at the Third USAF Symposium on Antennas, 1953.

R. E. Munson, “Microstrip Phased Array Antennas,” *Proc. of Twenty-Second Symp. on USAF Antenna Research and Development Program*, October 1972.

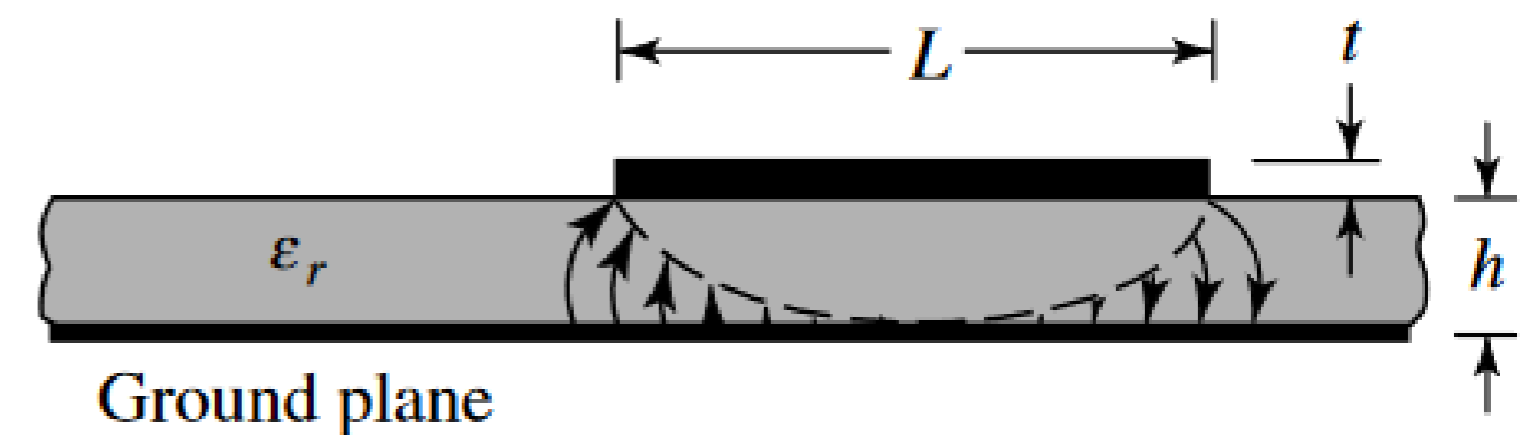
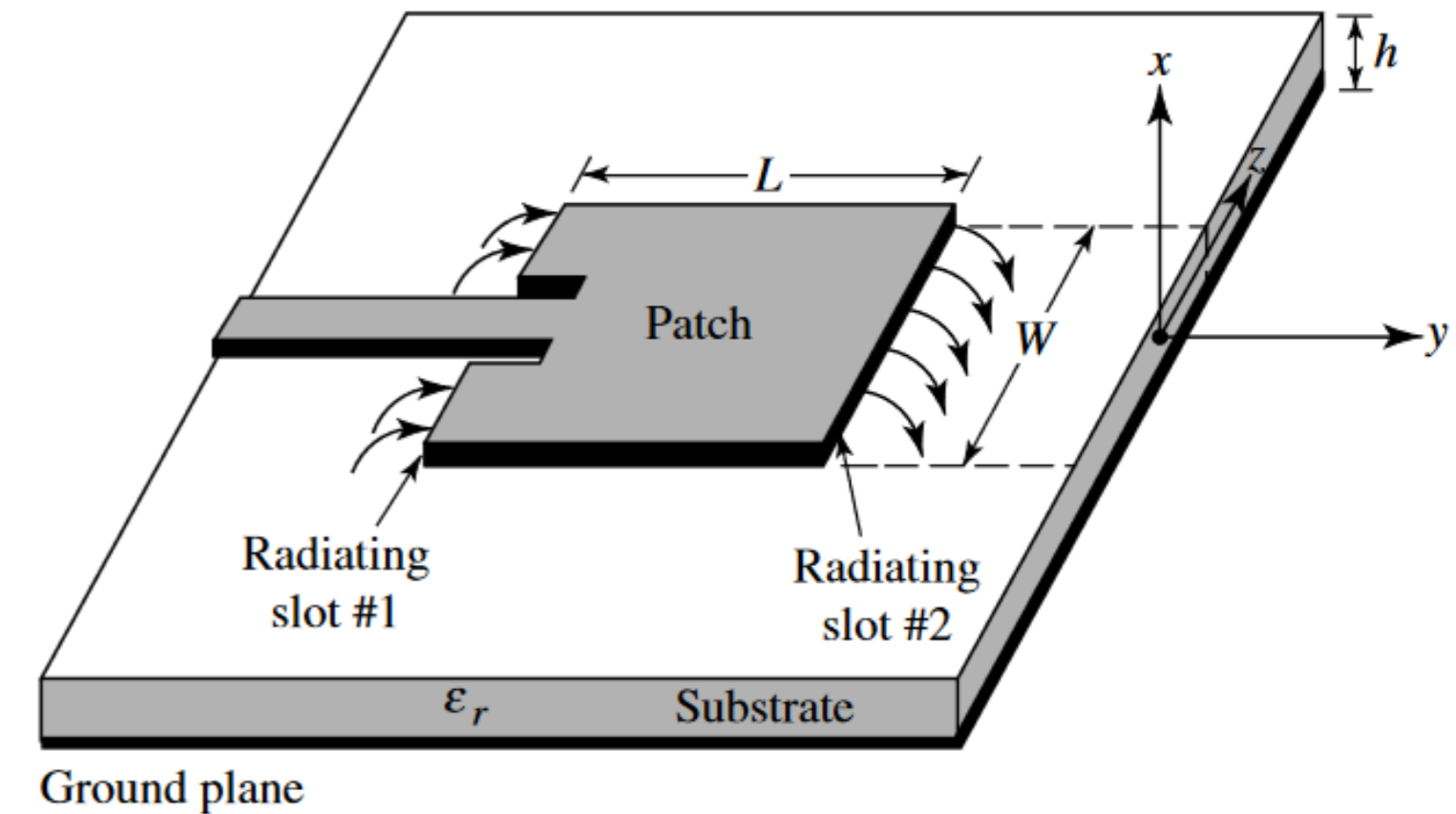
R. E. Munson, “Conformal Microstrip Antennas and Microstrip Phased Arrays,” *IEEE Trans. Antennas Propagat.*, vol. AP-22, no. 1 (January 1974): 74–78.

EPFL Microstrip Antenna

Microstrip antennas, as shown in the figure, consist of a very thin ($t \ll \lambda_0$, where λ_0 is the free-space wavelength) metallic strip (patch) placed a small fraction of a wavelength ($h \ll \lambda_0$, usually $0.003\lambda_0 \leq h \leq 0.05\lambda_0$) above a ground plane.

The microstrip patch is designed so its pattern maximum is normal to the patch (broadside radiator). This is accomplished by properly choosing the mode (field configuration) of excitation beneath the patch.

There are numerous substrates that can be used for the design of microstrip antennas, and their dielectric constants are usually in the range of $2.2 \leq \epsilon_r \leq 12$. The ones that are most desirable for good antenna performance are **thick** substrates whose dielectric constant is in the **lower** end of the range because they provide better efficiency, larger bandwidth, loosely bound fields for radiation into space, but at the expense of **larger** element size.



$$L \approx \lambda_d / 2 = \frac{1}{2} \frac{\lambda_0}{\sqrt{\epsilon_r}}$$

Advantages

- Low profile (can even be “conformal,” i.e. flexible to conform to a surface).
- Easy to fabricate (use etching and photolithography).
- Easy to feed (coaxial cable, microstrip line, etc.).
- Easy to incorporate with other microstrip circuit elements and integrate into systems.
- Patterns are somewhat hemispherical, with a moderate directivity (about 6-8 dB is typical).
- Easy to use in an array to increase the directivity.

Disadvantages

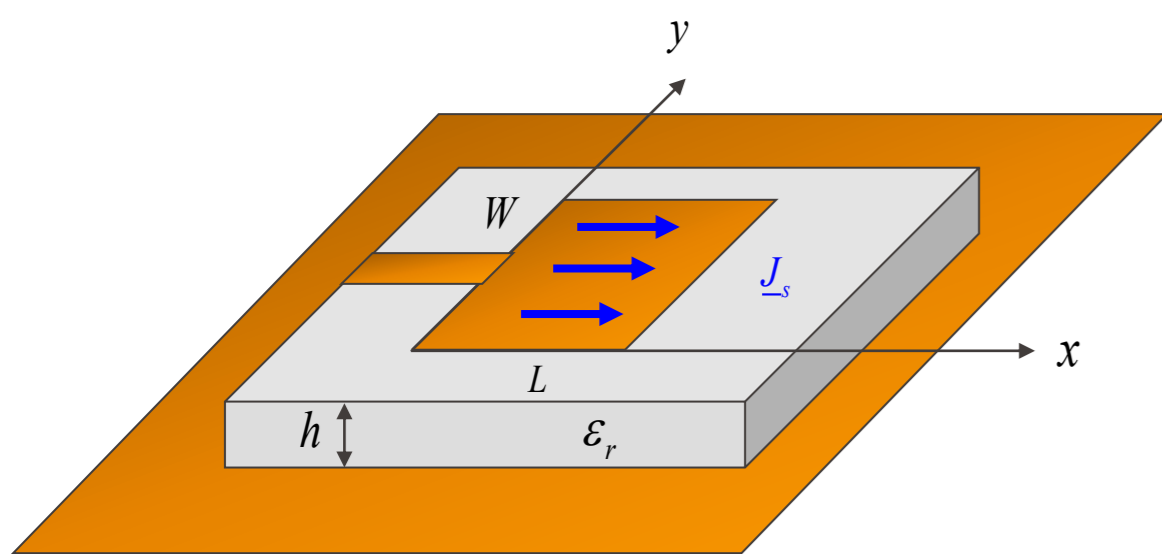
- Low bandwidth (but can be improved by a variety of techniques). Bandwidths of a few percent are typical. Bandwidth is roughly proportional to the substrate thickness and inversely proportional to the substrate permittivity.
- Efficiency may be lower than with other antennas. Efficiency is limited by conductor and dielectric losses*, and by surface-wave loss**.
- Only used at microwave frequencies and above (the substrate becomes too large at lower frequencies).
- Cannot handle extremely large amounts of power (dielectric breakdown).

* Conductor and dielectric losses become more severe for thinner substrates.

** Surface-wave losses become more severe for thicker substrates (unless air or foam is used).

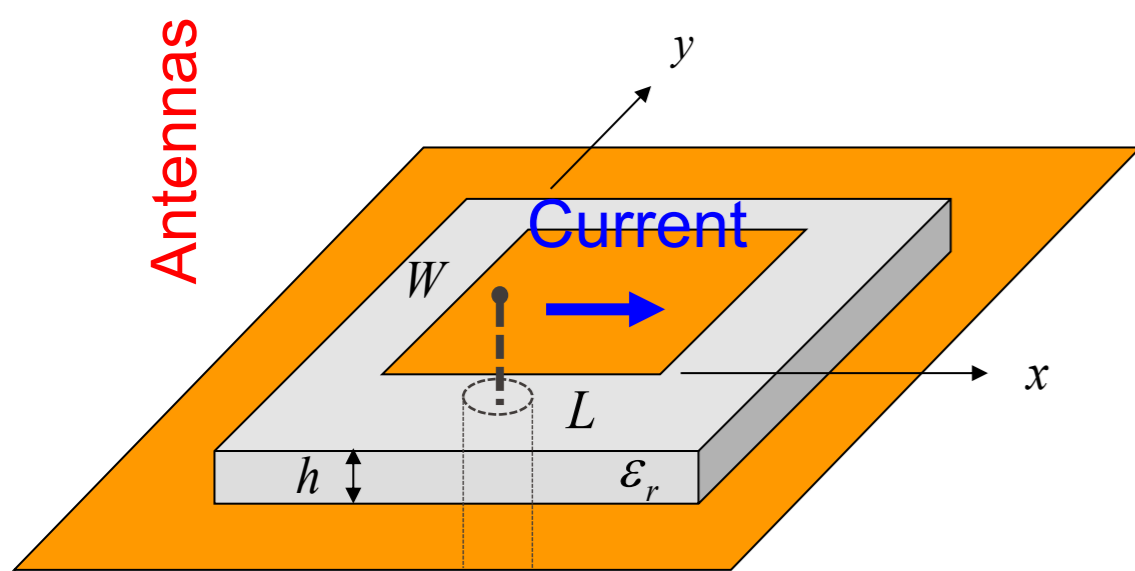
Microstrip Antenna

Feeding Method



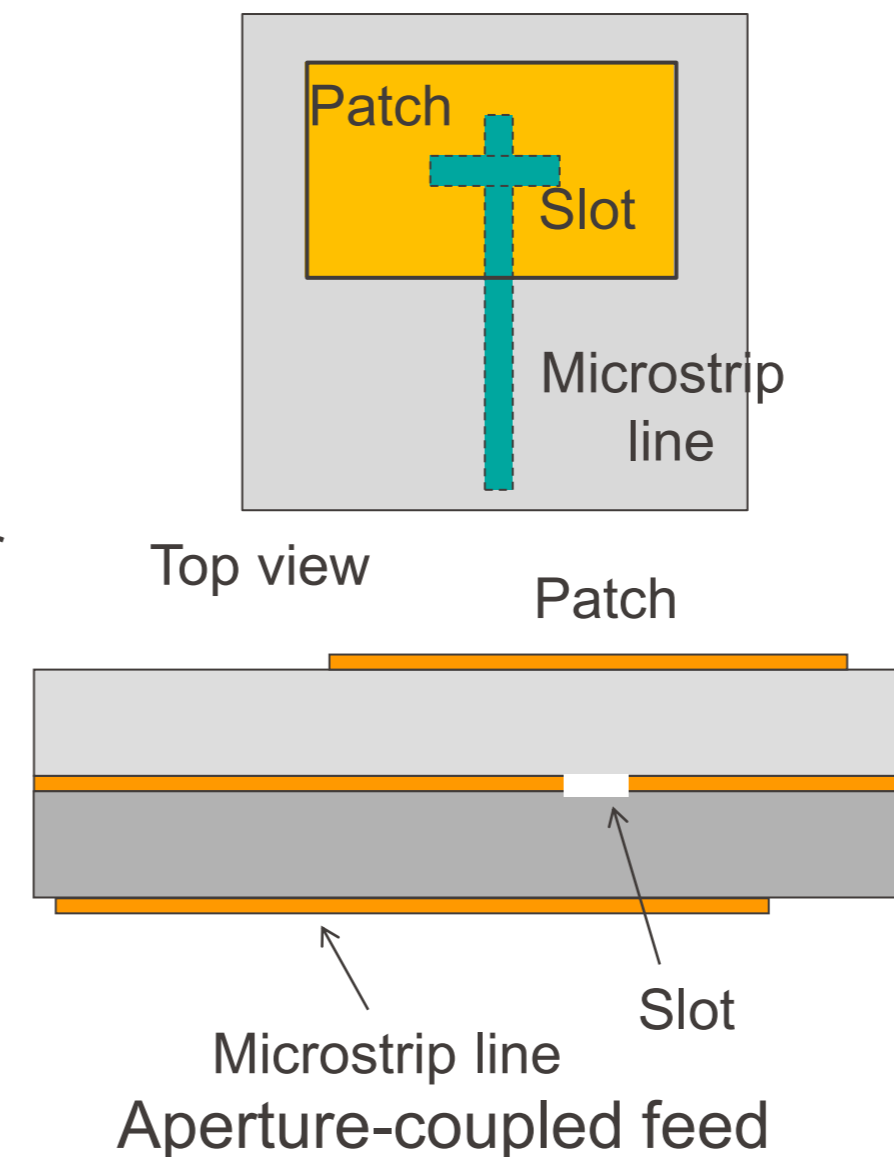
Microstrip line feed

The **microstrip feed** line is also a conducting strip, usually of much smaller width compared to the patch. The microstrip-line feed is easy to fabricate, simple to match by controlling the inset position and rather simple to model. However as the substrate thickness increases, surface waves and spurious feed radiation increase, which for practical designs limit the bandwidth (typically 2–5%). It suffers from inherent asymmetries which generate higher order modes which produce cross-polarized radiation.



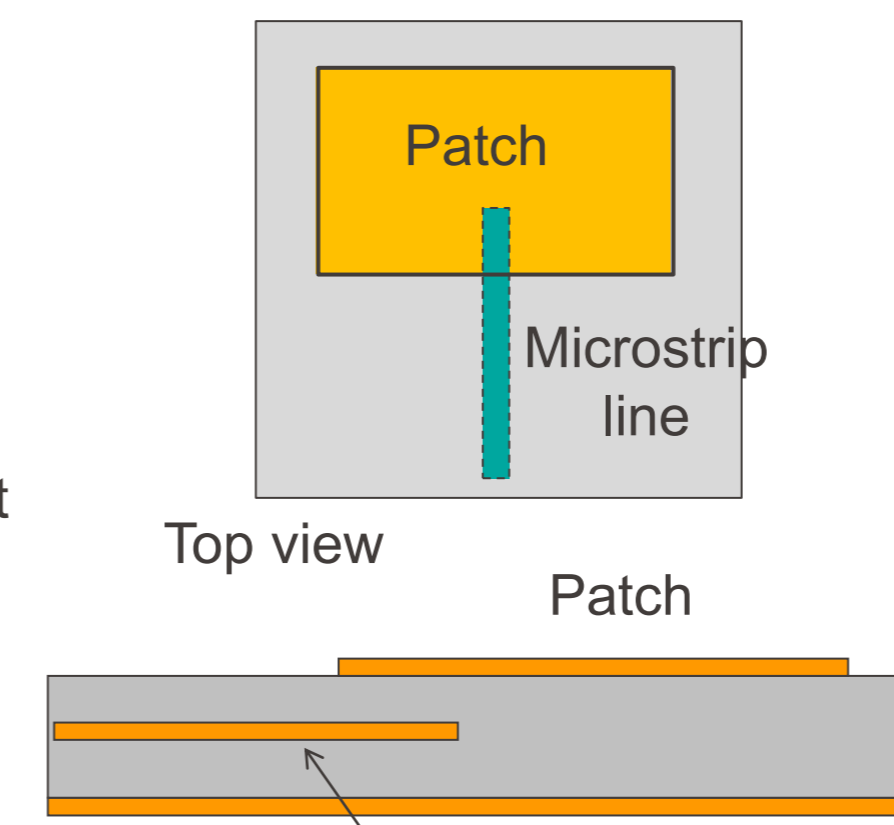
Probe feed, Coaxial Feed

Coaxial-line feeds, where the inner conductor of the coax is attached to the radiation patch while the outer conductor is connected to the ground plane, are also widely used. The coaxial probe feed is also easy to fabricate and match, and it has low spurious radiation. However, it also has narrow bandwidth and it is more difficult to model, especially for thick substrates ($h > 0.02\lambda_0$). It suffers from inherent asymmetries which generate higher order modes which produce cross-polarized radiation.



Aperture-coupled feed

The **aperture coupling** is the most difficult of all four to fabricate and it also has narrow bandwidth. However, it is somewhat easier to model and has moderate spurious radiation. The aperture coupling consists of two substrates separated by a ground plane. On the bottom side of the lower substrate there is a microstrip feed line whose energy is coupled to the patch through a slot on the ground plane separating the two substrates. This arrangement allows independent optimization of the feed mechanism and the radiating element. Typically a high dielectric material is used for the bottom substrate, and thick low dielectric constant material for the top substrate. The ground plane between the substrates also isolates the feed from the radiating element and minimizes interference of spurious radiation for pattern formation and polarization purity.



Proximity-coupled feed

The **proximity coupling** has the largest bandwidth (as high as 13 percent), is somewhat easy to model and has low spurious radiation. However its fabrication is somewhat more difficult. The length of the feeding stub and the width-to-line ratio of the patch can be used to control the match.

Microstrip Antenna

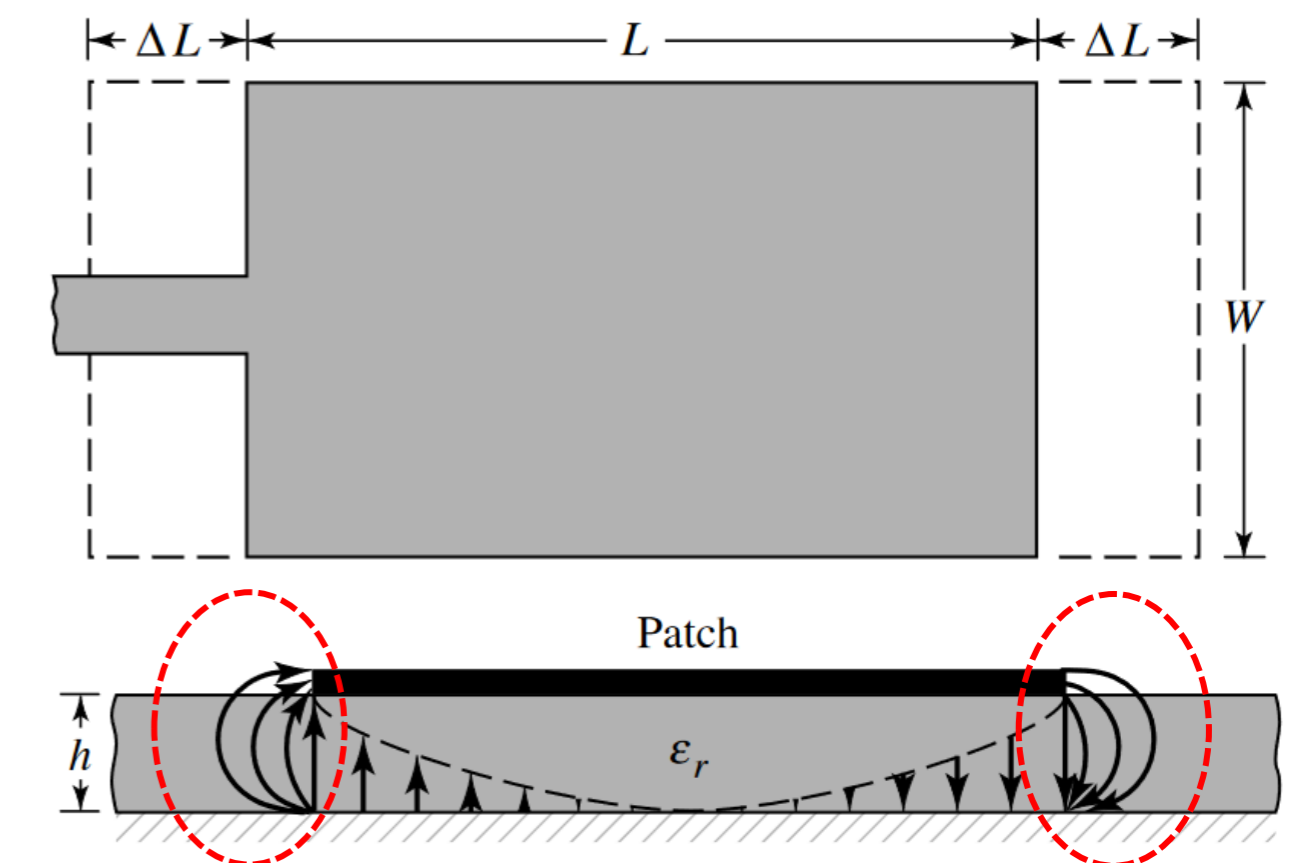
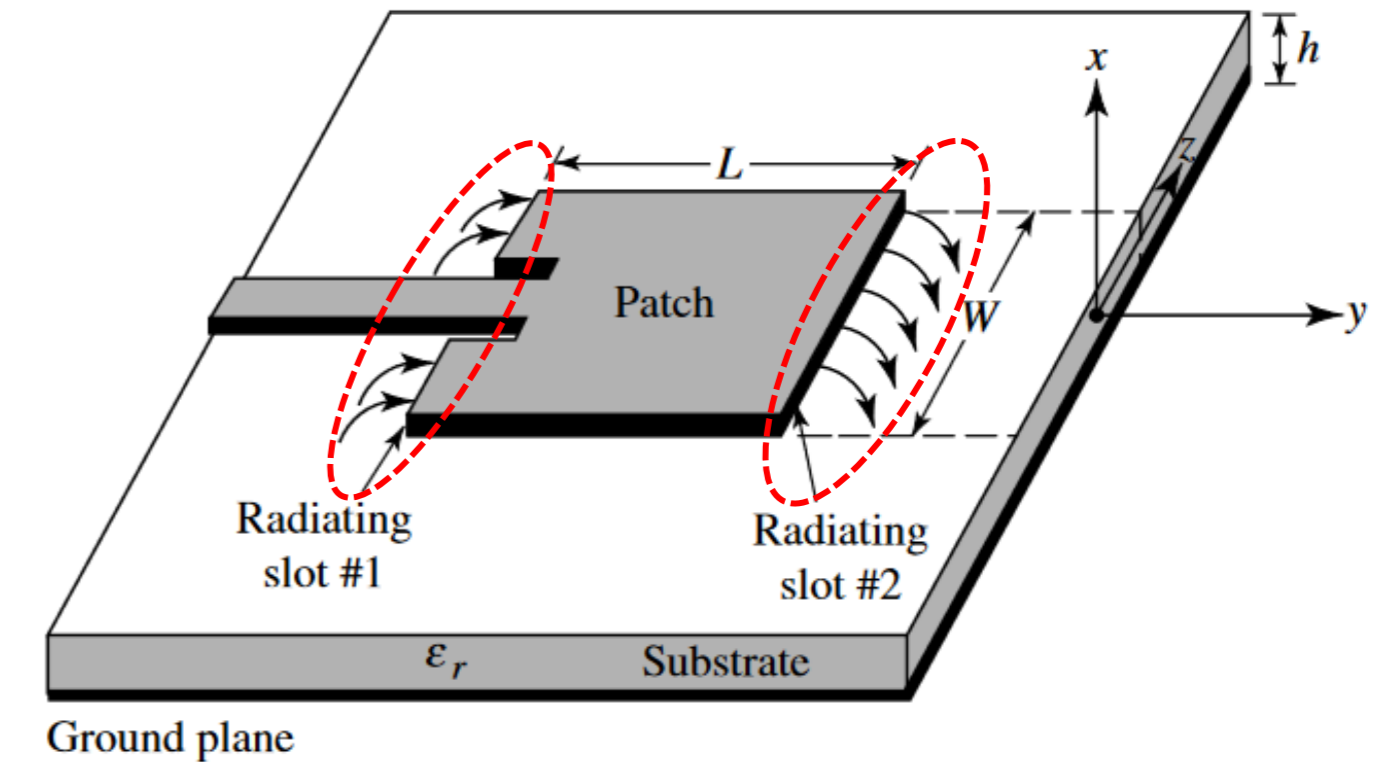
Effective Length

Because of the fringing effects, electrically the patch of the microstrip antenna looks greater than its physical dimensions. For the principal E-plane (xy-plane), this is demonstrated in the figure where the dimensions of the patch along its length have been extended on each end by a distance ΔL , which is a function of the effective dielectric constant ϵ_{reff} and the width-to-height ratio (W/h). A very popular and practical approximate relation for the normalized extension of the length is

$$\frac{\Delta L}{h} = 0.412 \frac{(\epsilon_{\text{reff}} + 0.3) \left(\frac{W}{h} + 0.264 \right)}{(\epsilon_{\text{reff}} - 0.258) \left(\frac{W}{h} + 0.8 \right)}$$

Since the length of the patch has been extended by ΔL on each side, the effective length of the patch is now ($L = \lambda/2$ for dominant TM_{010} mode with no fringing)

$$L_{\text{eff}} = L + 2\Delta L$$



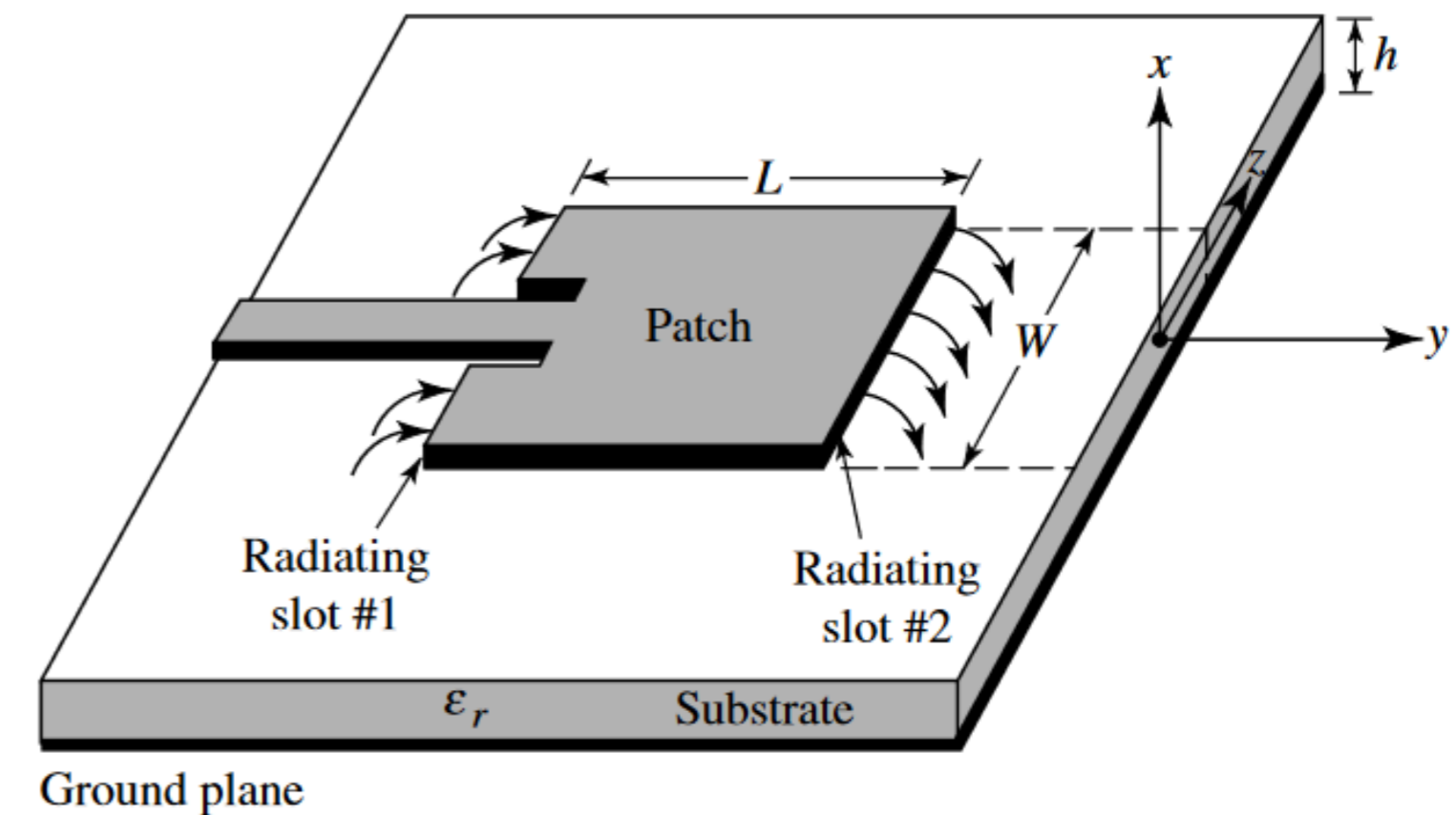
Physical and effective lengths of rectangular microstrip patch

Based on the simplified formulation that has been described, a design procedure is outlined which leads to practical designs of rectangular microstrip antennas. The procedure assumes that the specified information includes the dielectric constant of the substrate (ϵ_r), the resonant frequency (f_r), and the height of the substrate h , and v_0 is the free space velocity of wave. The procedure is as follows:

- Choosing the dielectric material (Substrate)
- Determining the W and L as a function of desired frequency

$$W = \frac{1}{2f_r \sqrt{\mu_0 \epsilon_0}} \sqrt{\frac{2}{\epsilon_r + 1}} = \frac{v_0}{2f_r} \sqrt{\frac{2}{\epsilon_r + 1}}$$

$$L = \frac{1}{2f_r \sqrt{\epsilon_{\text{reff}}} \sqrt{\mu_0 \epsilon_0}} - 2\Delta L$$



The equivalent admittance of slot #1, based on an infinitely wide, uniform slot is given by

$$Y_1 = G_1 + jB_1$$

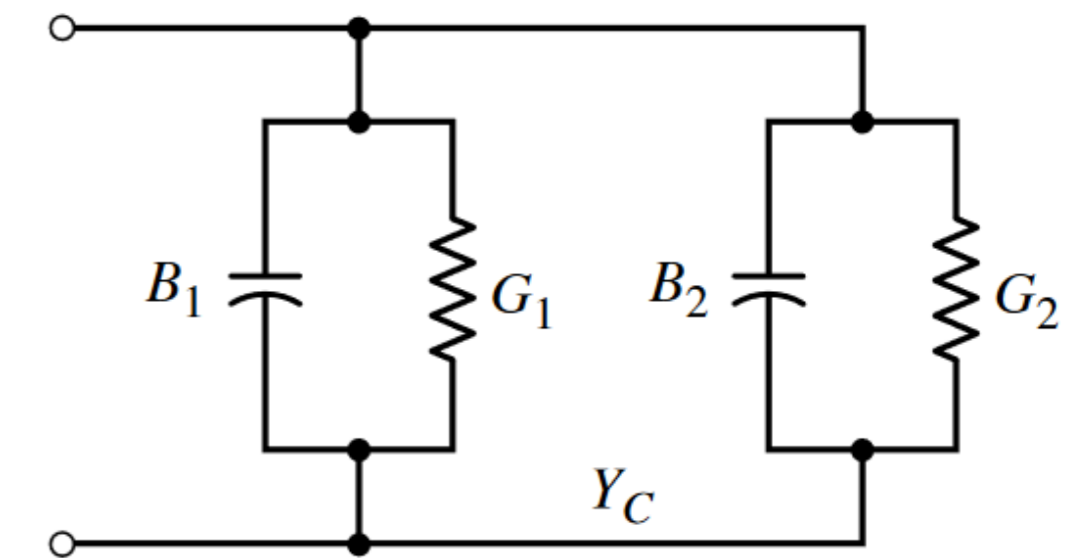
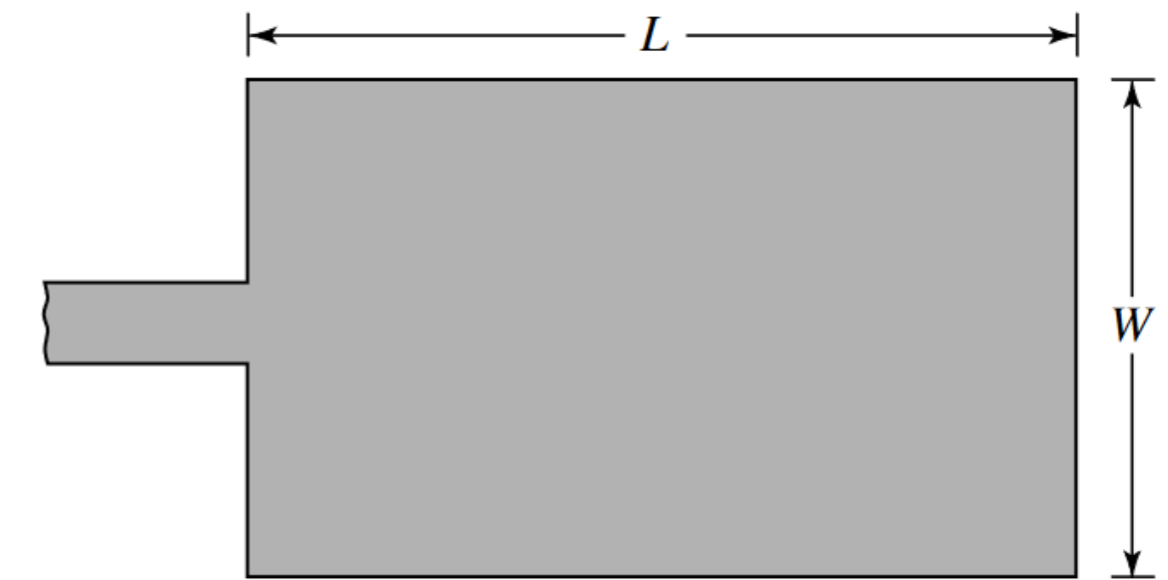
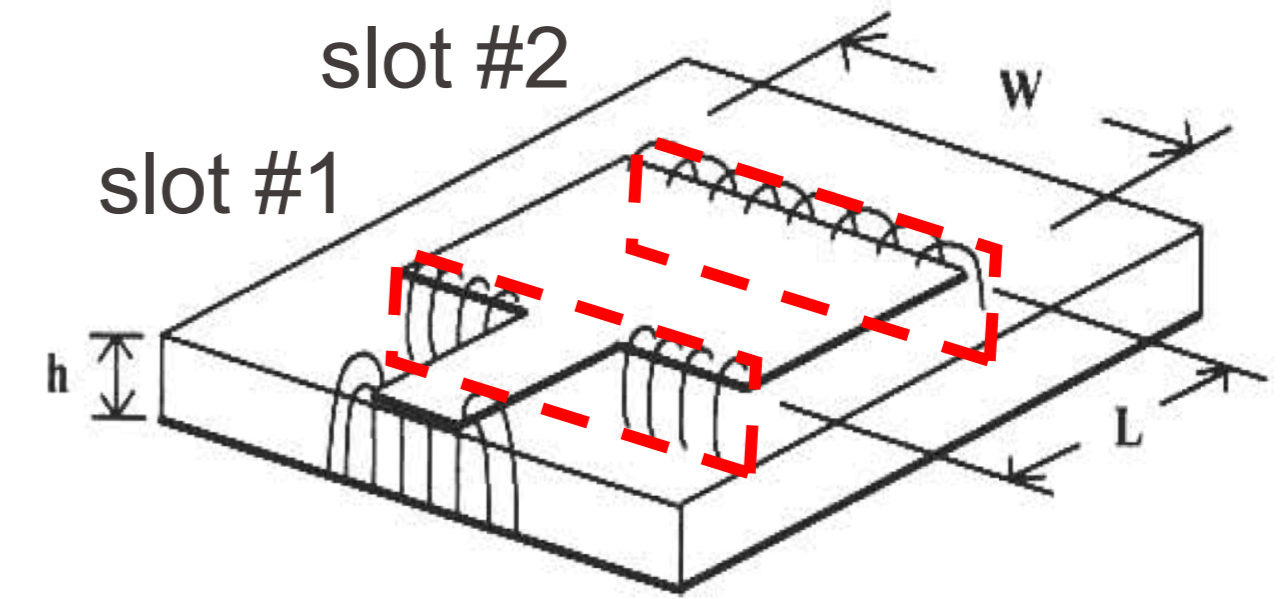
where for a slot of finite width W

$$G_1 = \frac{W}{120\lambda_0} \left[1 - \frac{1}{24}(k_0h)^2 \right] \quad \frac{h}{\lambda_0} < \frac{1}{10}$$

$$B_1 = \frac{W}{120\lambda_0} [1 - 0.636 \ln(k_0h)] \quad \frac{h}{\lambda_0} < \frac{1}{10}$$

Since slot #2 is identical to slot #1, its equivalent admittance is

$$Y_2 = Y_1, \quad G_2 = G_1, \quad B_2 = B_1$$



Each radiating slot is represented by a parallel equivalent admittance Y (with conductance G and susceptance B).

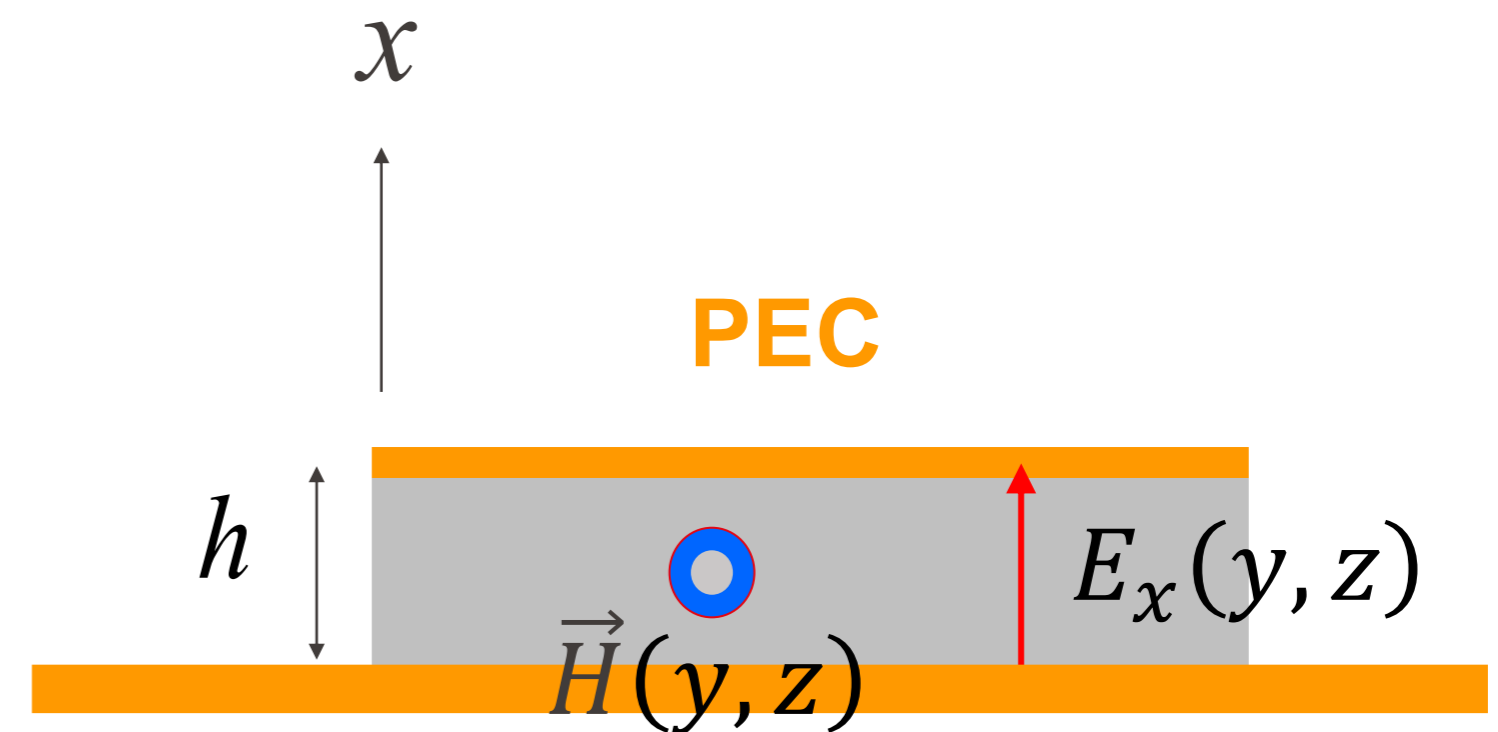
On patch and ground plane: $E_t = 0 \rightarrow \vec{E} = \hat{x}E_x$

Inside the patch cavity, because of the thin substrate, the electric field vector is approximately independent of x . Hence:

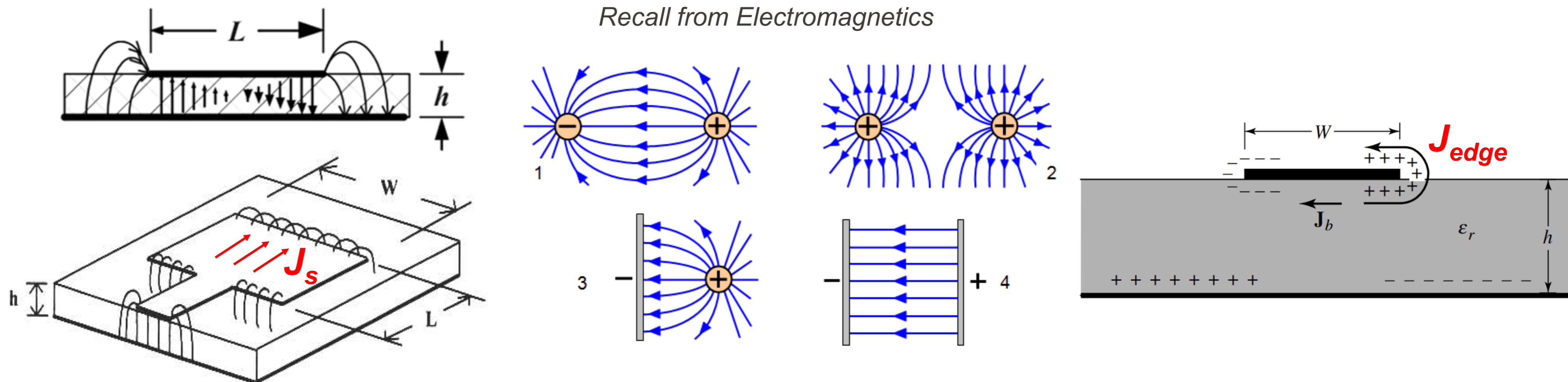
$$\vec{E}(x, y, z) \approx \hat{x}E_x(y, z)$$

Magnetic field inside patch cavity:

$$\begin{aligned} \vec{H} &\approx -\frac{1}{j\omega\mu} \nabla \times E_x(y, z) \\ &= -\frac{1}{j\omega\mu} \nabla \times (\hat{x}E_x(y, z)) \\ &= -\frac{1}{j\omega\mu} (-\hat{x} \times \nabla E_x(y, z)) \end{aligned}$$

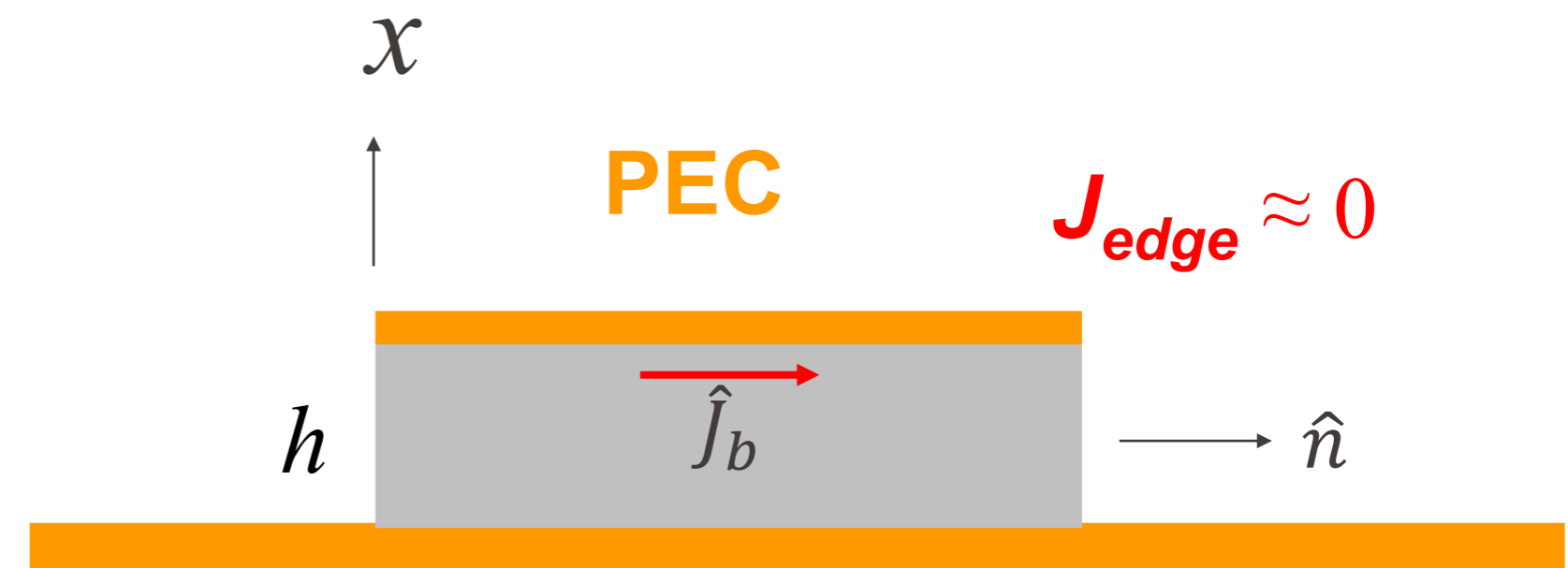


The magnetic field is purely **horizontal**.
(The mode is TM_x)



When a microstrip patch is energized, a charge distribution is established on the upper and lower surfaces of the patch, as well as on the surface of the ground plane. The charge distribution is controlled by two mechanisms; an **attractive** and a **repulsive** mechanism. The **attractive** mechanism is between the corresponding opposite charges on the bottom side of the patch and the ground plane, which tends to maintain the charge concentration on the bottom of the patch. The **repulsive** mechanism is between like charges on the bottom surface of the patch, which tends to push some charges from the bottom of the patch, around its edges, to its top surface. The movement of these charges creates corresponding current densities J_b and J_{edge} , at the bottom and top surfaces of the patch, respectively, as shown in the figure.

Since for most practical microstrips the height-to-width ratio is very small, the attractive mechanism dominates and most of the charge concentration and current flow remain underneath the patch. A small amount of current flows around the edges of the patch to its top surface. However, this current flow decreases as the height-to-width ratio decreases. In the limit, the current flow to the top would be **zero**.



The electric current on the patch

$$\hat{J}_b = -\hat{x} \times \vec{H}(y, z)$$

The patch edge acts as an approximate **open circuit** :

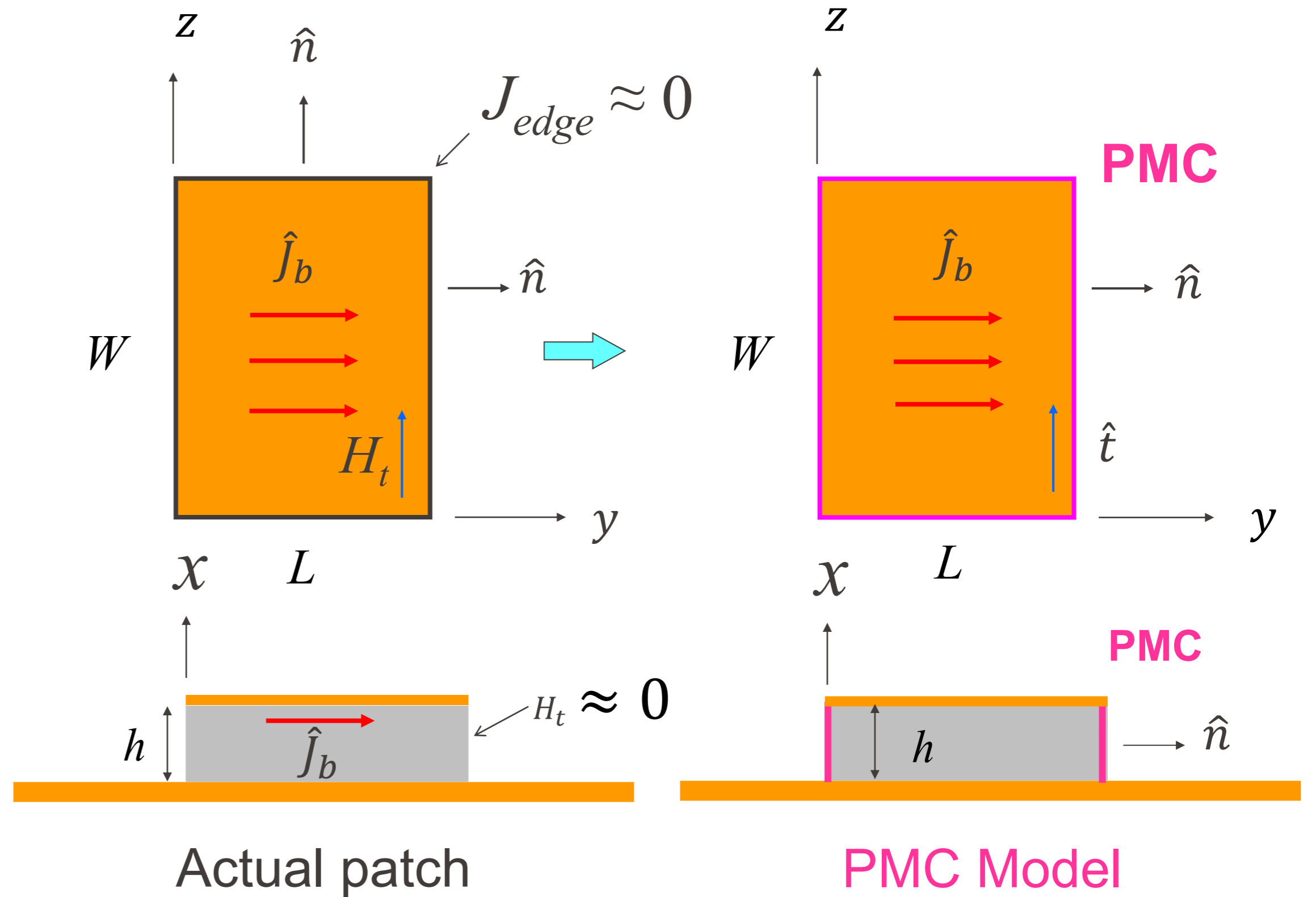
$$J_{edge} = \hat{n} \times \vec{H}(y, z) = 0$$

Since

$$\vec{H} = H_n + H_t$$

$$\hat{n} \times \vec{H} = \hat{n} \times H_n + \hat{n} \times H_t = \hat{n} \times H_t$$

$$\Rightarrow H_t = 0 \quad \boxed{\text{PMC}}$$



Antennas

On PMC patch edge: $\hat{n} \times \vec{H}(y, z) = 0$

$$\vec{H}(y, z) = \frac{1}{j\omega\mu} (\hat{x} \times \nabla E_x(y, z))$$

Hence,

$$H_t = \vec{H} \cdot \hat{t} = \frac{1}{j\omega\mu} (\hat{x} \times \nabla E_x(y, z)) \cdot \hat{t}$$

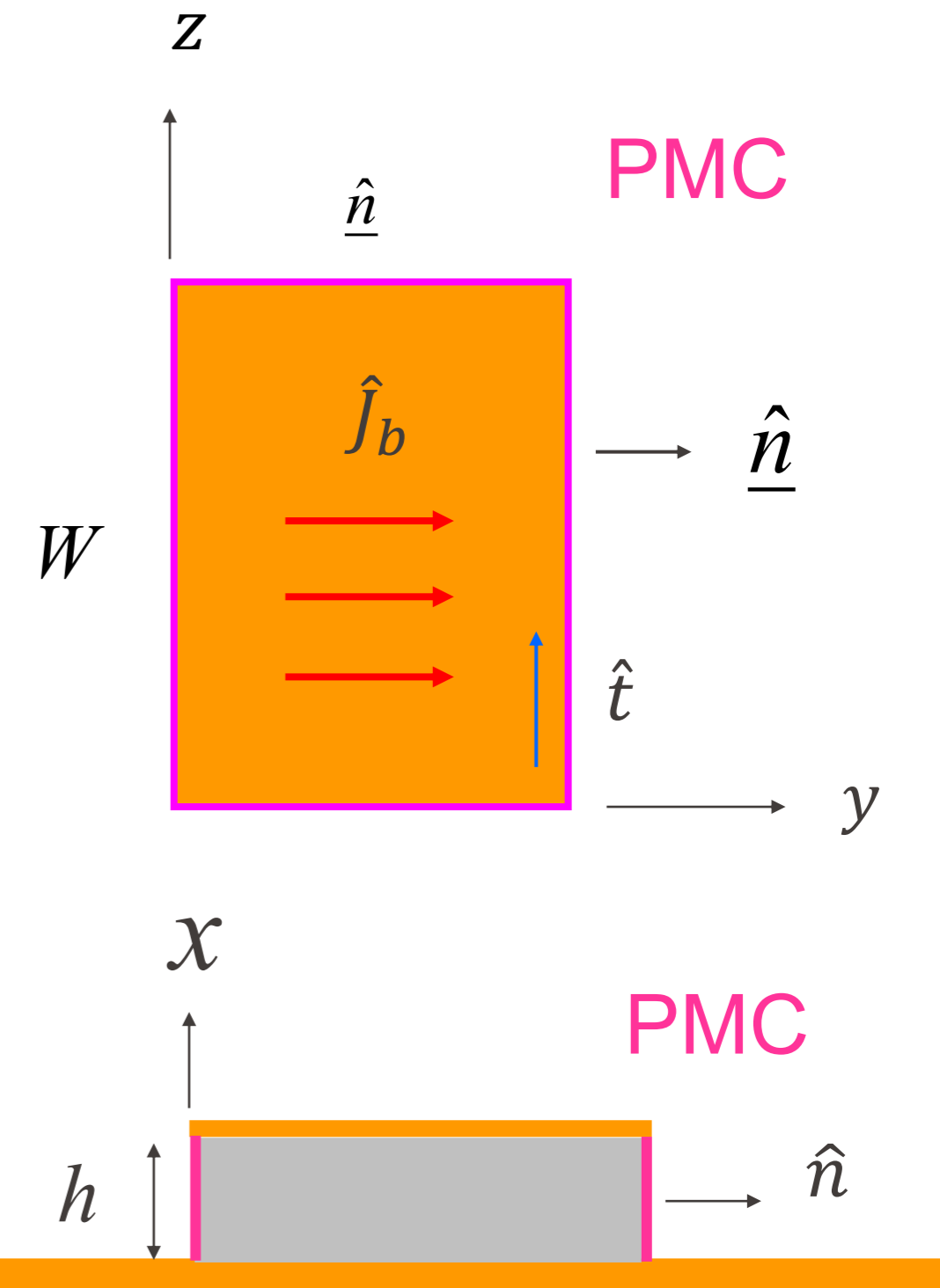
Since,

$$(\hat{x} \times \nabla E_x(y, z)) \cdot \hat{t} = \nabla E_x(y, z) \cdot (\hat{t} \times \hat{x})$$

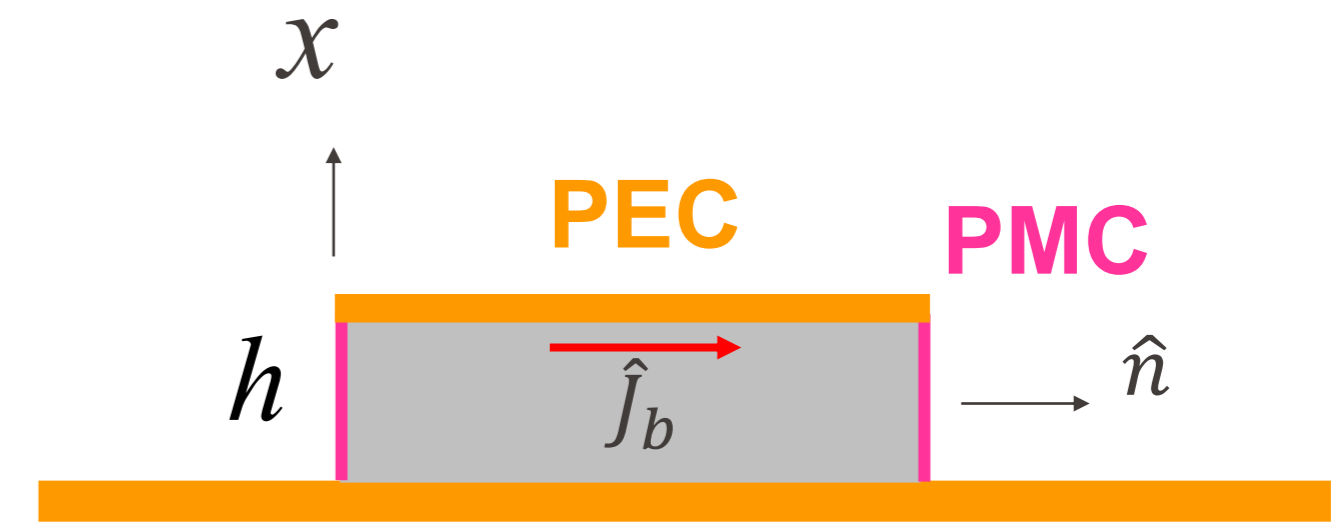
and

$$\hat{t} \times \hat{x} = \hat{n} \quad \frac{\partial f}{\partial n} = \nabla f \cdot \hat{n}$$

$$H_t = \frac{1}{j\omega\mu} \nabla E_x(y, z) \cdot \hat{n} = \frac{1}{j\omega\mu} \frac{\partial E_x}{\partial n} = 0 \quad \rightarrow \quad \frac{\partial E_x}{\partial n} = 0 \quad (\text{Neumann B.C.})$$



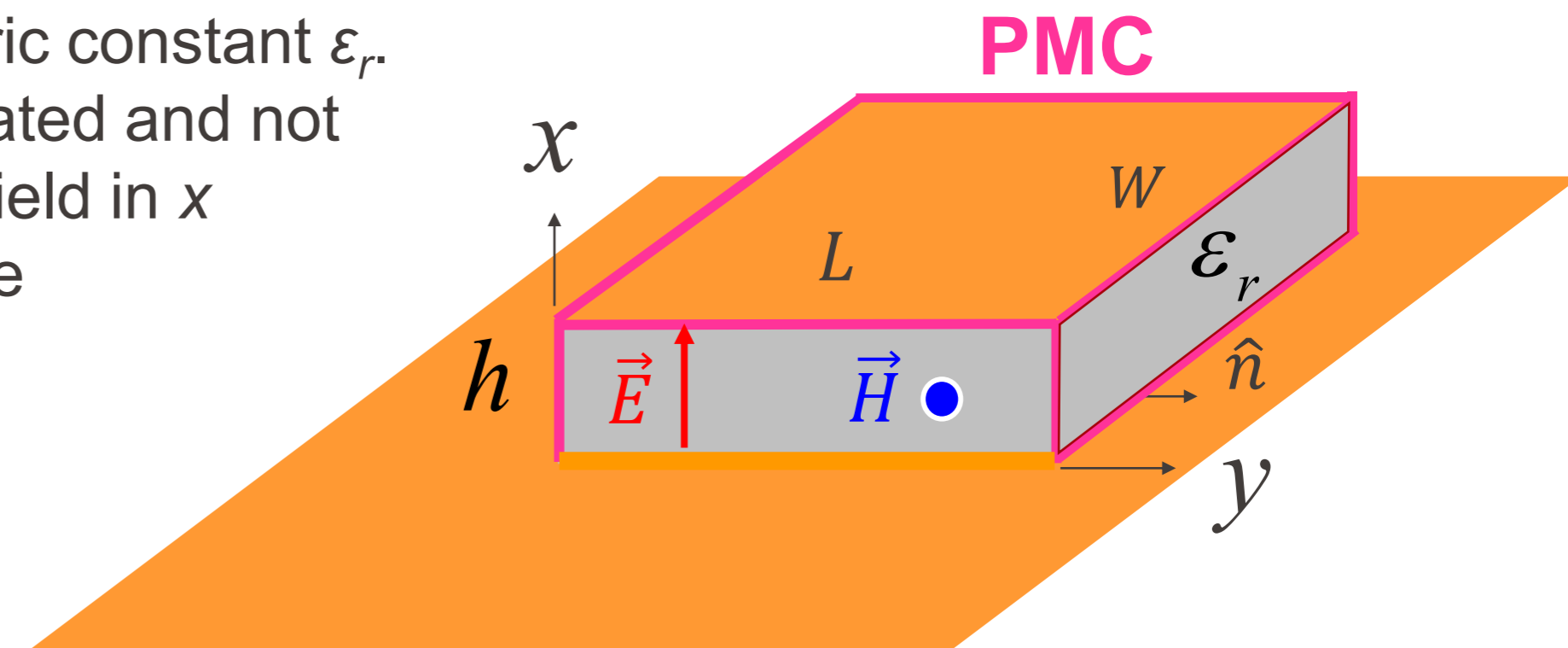
This would allow the four side walls to be modeled as **perfect magnetic** conducting surfaces which ideally would not disturb the magnetic field and, in turn, the electric field distributions beneath the patch. Since in practice there is a finite height-to-width ratio, although small, the tangential magnetic fields at the edges would not be exactly zero. However, since they will be small, a good approximation to the cavity model is to treat the side walls as perfectly magnetic conducting. This model produces good normalized electric and magnetic field distributions (modes) beneath the patch.



- The patch acts approximately as a resonant cavity (with perfect electric conductor (**PEC**) walls on top and bottom, and perfect magnetic conductor (**PMC**) walls on the edges).
- In a cavity, only **certain modes** are allowed to exist, at different resonance frequencies.
- If the antenna is excited at a resonance frequency, a strong field is set up inside the cavity, and a strong current on the (bottom) surface of the patch. This produces significant radiation (a good antenna).

The field configurations within the cavity can be found using the vector potential approach. The volume beneath the patch can be treated as a rectangular cavity loaded with a dielectric material with dielectric constant ϵ_r . The dielectric material of the substrate is assumed to be truncated and not extended beyond the edges of the patch. Since the magnetic field in x direction is zero (TM^x), the **vector potential** A_x must satisfy the homogeneous wave equation of

$$\nabla^2 A_x + k^2 A_x = 0$$



Rectangular microstrip patch geometry

whose solution is written in general, using the separation of variables, as

$$A_x = [A_1 \cos(k_x x) + B_1 \sin(k_x x)][A_2 \cos(k_y y) + B_2 \sin(k_y y)][A_3 \cos(k_z z) + B_3 \sin(k_z z)]$$

where k_x , k_y and k_z are the wave numbers along the x , y , and z directions, respectively. These will be determined subject to the boundary conditions.

The electric and magnetic fields within the cavity are related to the vector potential A_x by

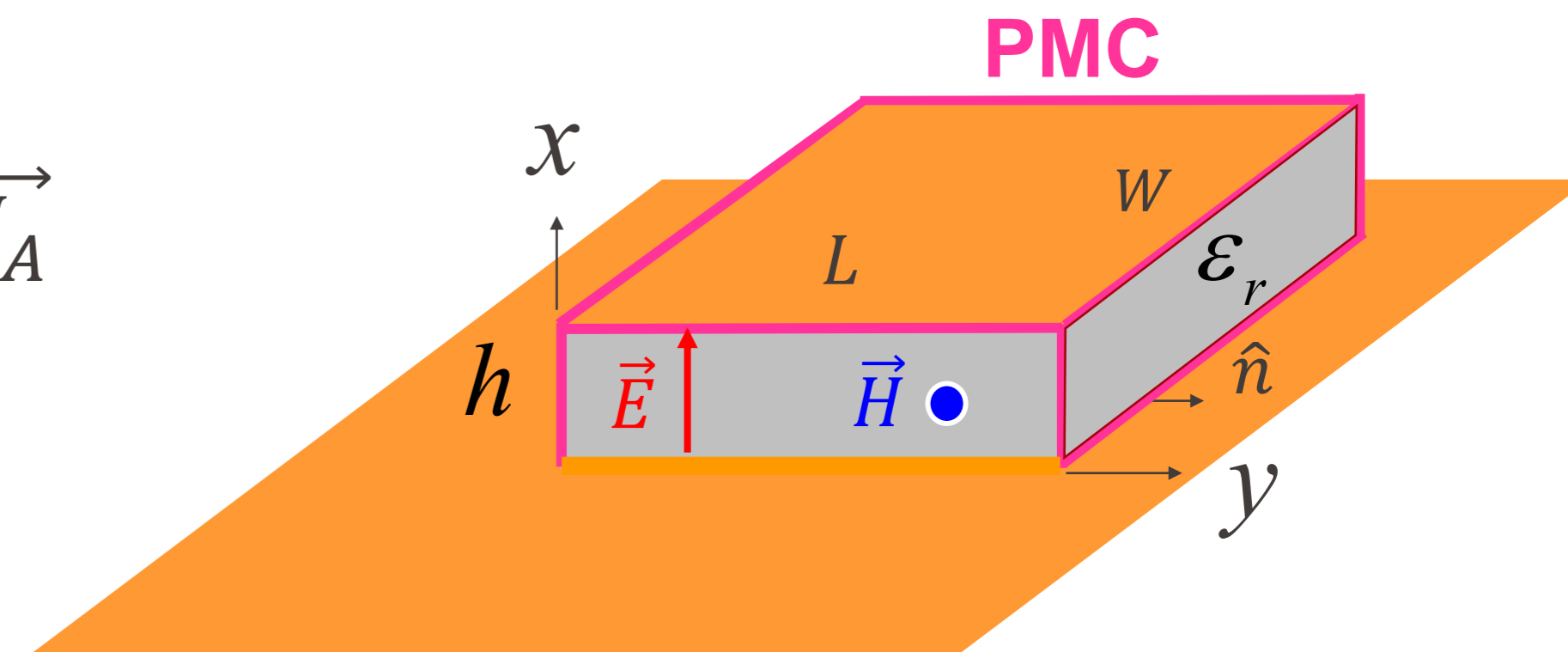
$$\vec{H}_A = \frac{1}{\mu} \nabla \times \vec{A} \quad \vec{E}_A = \frac{1}{j\omega\epsilon} \nabla \times \vec{H}_A$$

Thus

$$E_x = -j \frac{1}{\omega\mu\epsilon} \left(\frac{\partial^2}{\partial x^2} + k^2 \right) A_x \quad H_x = 0$$

$$E_y = -j \frac{1}{\omega\mu\epsilon} \frac{\partial^2 A_x}{\partial x \partial y} \quad H_y = \frac{1}{\mu} \frac{\partial A_x}{\partial z}$$

$$E_z = -j \frac{1}{\omega\mu\epsilon} \frac{\partial^2 A_x}{\partial x \partial z} \quad H_z = -\frac{1}{\mu} \frac{\partial A_x}{\partial y}$$



Rectangular microstrip patch geometry

The boundary conditions of

$$E_y(x' = 0, 0 \leq y' \leq L, 0 \leq z' \leq W) = E_y(x' = h, 0 \leq y' \leq L, 0 \leq z' \leq W) = 0$$

$$H_y(0 \leq x' \leq h, 0 \leq y' \leq L, z' = 0) = H_y(0 \leq x' \leq h, 0 \leq y' \leq L, z' = W) = 0$$

$$H_z(0 \leq x' \leq h, y' = 0, 0 \leq z' \leq W) = H_z(0 \leq x' \leq h, y' = L, 0 \leq z' \leq W) = 0$$



Cavity Model B.C.

Applying the boundary condition to A_x

$$A_x = [A_1 \cos(k_x x) + \cancel{B_1} \sin(k_x x)][A_2 \cos(k_y y) + \cancel{B_2} \sin(k_y y)][A_3 \cos(k_z z) + \cancel{B_3} \sin(k_z z)]$$

$$\rightarrow k_x = \frac{m\pi}{h}, \quad m = 0, 1, 2, \dots$$

$$\rightarrow k_y = \frac{n\pi}{L}, \quad n = 0, 1, 2, \dots$$

$$\rightarrow k_z = \frac{p\pi}{W}, \quad p = 0, 1, 2, \dots$$

* The primed coordinates x' , y' , z' are used to represent the fields within the cavity.

Thus the final form for the vector potential A_x within the cavity is

$$A_x = A_{mnp} \cos(k_x x') \cos(k_y y') \cos(k_z z')$$

Substituting A_x into \mathbf{E} and \mathbf{H} , the electric and magnetic fields within the cavity are written as

$$E_x = -j \frac{1}{\omega \mu \epsilon} \left(\frac{\partial^2}{\partial x^2} + k^2 \right) A_x$$

$$E_y = -j \frac{1}{\omega \mu \epsilon} \frac{\partial^2 A_x}{\partial x \partial y}$$

$$E_z = -j \frac{1}{\omega \mu \epsilon} \frac{\partial^2 A_x}{\partial x \partial z}$$

$$H_x = 0$$

$$H_y = \frac{1}{\mu} \frac{\partial A_x}{\partial z}$$

$$H_z = -\frac{1}{\mu} \frac{\partial A_x}{\partial y}$$

Substituting \mathbf{A}_x into \mathbf{E} and \mathbf{H} , the electric and magnetic fields within the cavity are written as

$$E_x = -j \frac{(k^2 - k_x^2)}{\omega\mu\epsilon} A_{mnp} \cos(k_x x') \cos(k_y y') \cos(k_z z')$$

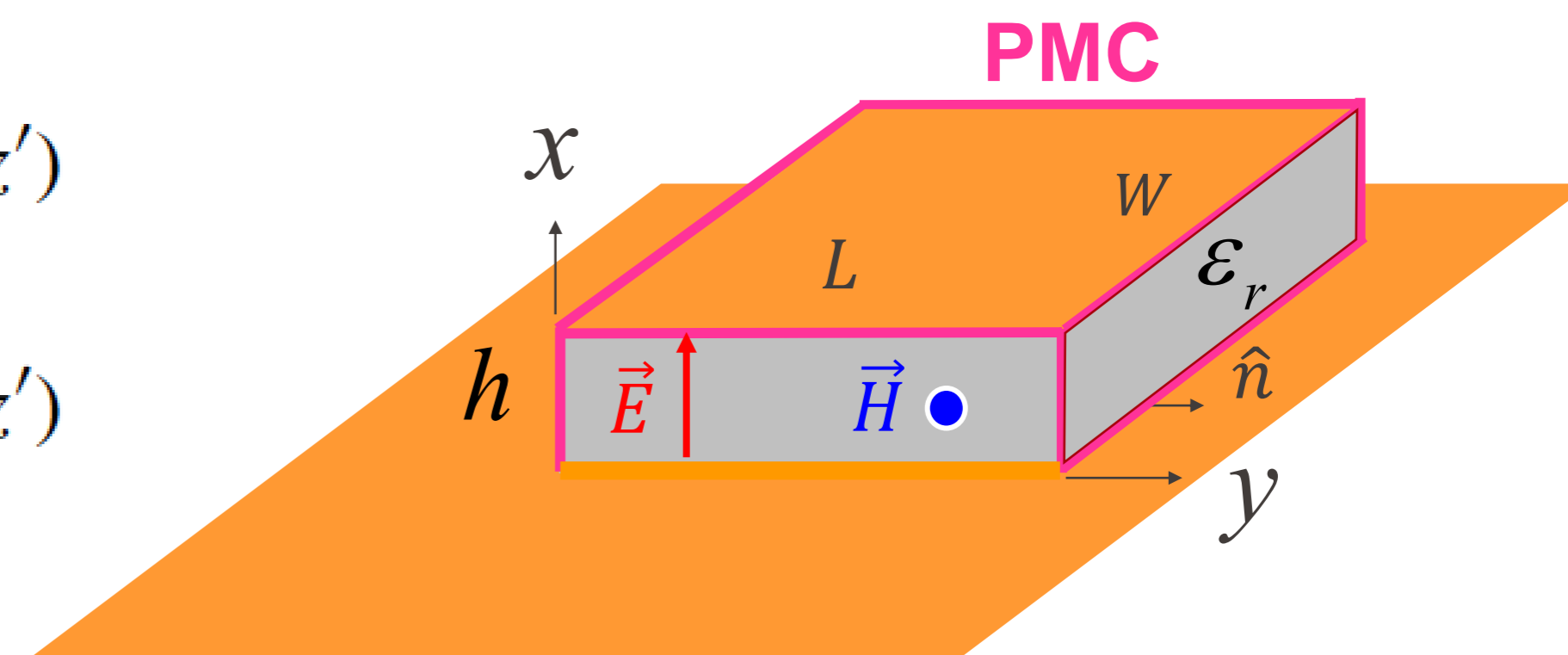
$$E_y = -j \frac{k_x k_y}{\omega\mu\epsilon} A_{mnp} \sin(k_x x') \sin(k_y y') \cos(k_z z')$$

$$E_z = -j \frac{k_x k_z}{\omega\mu\epsilon} A_{mnp} \sin(k_x x') \cos(k_y y') \sin(k_z z')$$

$$H_x = 0$$

$$H_y = -\frac{k_z}{\mu} A_{mnp} \cos(k_x x') \cos(k_y y') \sin(k_z z')$$

$$H_z = \frac{k_y}{\mu} A_{mnp} \cos(k_x x') \sin(k_y y') \cos(k_z z')$$



Rectangular microstrip patch geometry

Since the wavenumbers k_x , k_y and k_z are subject to the constraint equation

$$k_x^2 + k_y^2 + k_z^2 = \left(\frac{m\pi}{h}\right)^2 + \left(\frac{n\pi}{L}\right)^2 + \left(\frac{p\pi}{W}\right)^2 = k_r^2 = \omega_r^2 \mu \epsilon$$

the resonant frequencies for the cavity are given by

$$(f_r)_{mnp} = \frac{1}{2\pi \sqrt{\mu \epsilon}} \sqrt{\left(\frac{m\pi}{h}\right)^2 + \left(\frac{n\pi}{L}\right)^2 + \left(\frac{p\pi}{W}\right)^2}$$

Cavity Model

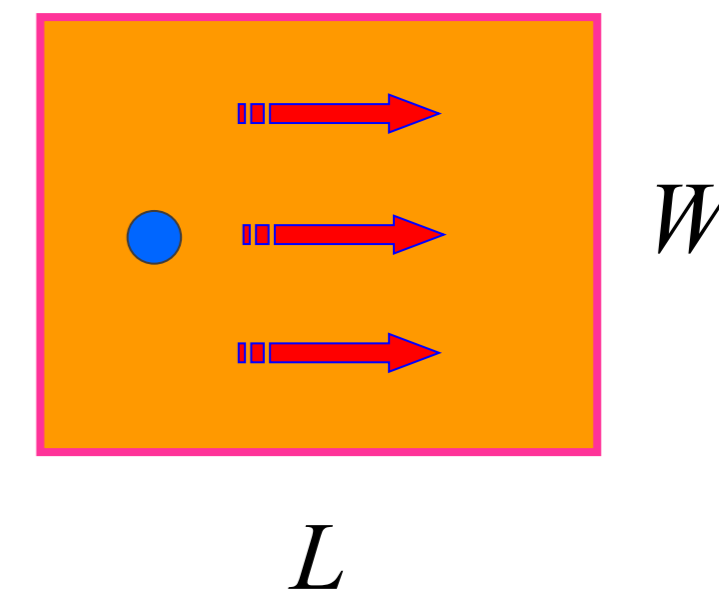
Resonance Frequencies

$$f_{mn} = \frac{1}{2\pi\sqrt{\mu\epsilon}} \sqrt{\left(\frac{m\pi}{h}\right)^2 + \left(\frac{n\pi}{L}\right)^2 + \left(\frac{p\pi}{W}\right)^2}$$

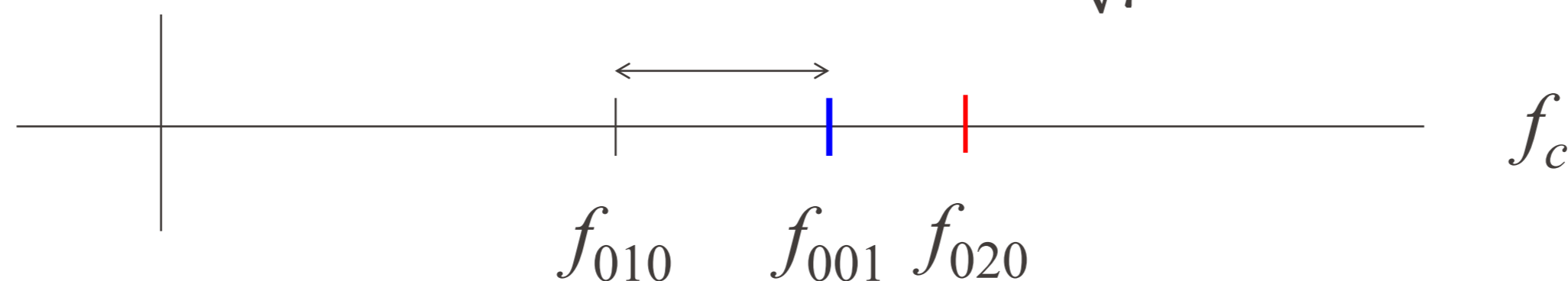
$$f_{010} = \frac{1}{2\sqrt{\mu\epsilon}} \left(\frac{1}{L}\right)$$

$$f_{001} = \frac{1}{2\sqrt{\mu\epsilon}} \left(\frac{1}{W}\right)$$

$$f_{020} = \frac{1}{2\sqrt{\mu\epsilon}} \left(\frac{2}{L}\right)$$

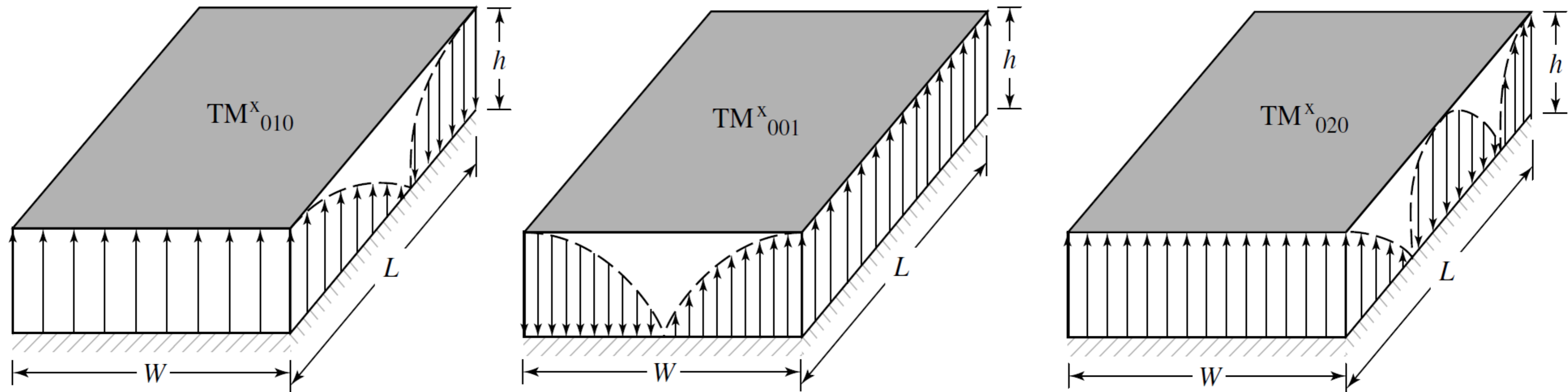


$$BW \propto |f_{010} - f_{001}| = \frac{1}{2\sqrt{\mu\epsilon}} \left(\frac{1}{L} - \frac{1}{W}\right)$$



Cavity Model

Resonance Frequencies



$$f_{010} = \frac{1}{2\sqrt{\mu\epsilon}} \left(\frac{1}{L} \right) = \frac{v_0}{2\sqrt{\epsilon_r}} \left(\frac{1}{L} \right)$$

$$f_{001} = \frac{1}{2\sqrt{\mu\epsilon}} \left(\frac{1}{W} \right) = \frac{v_0}{2\sqrt{\epsilon_r}} \left(\frac{1}{W} \right)$$

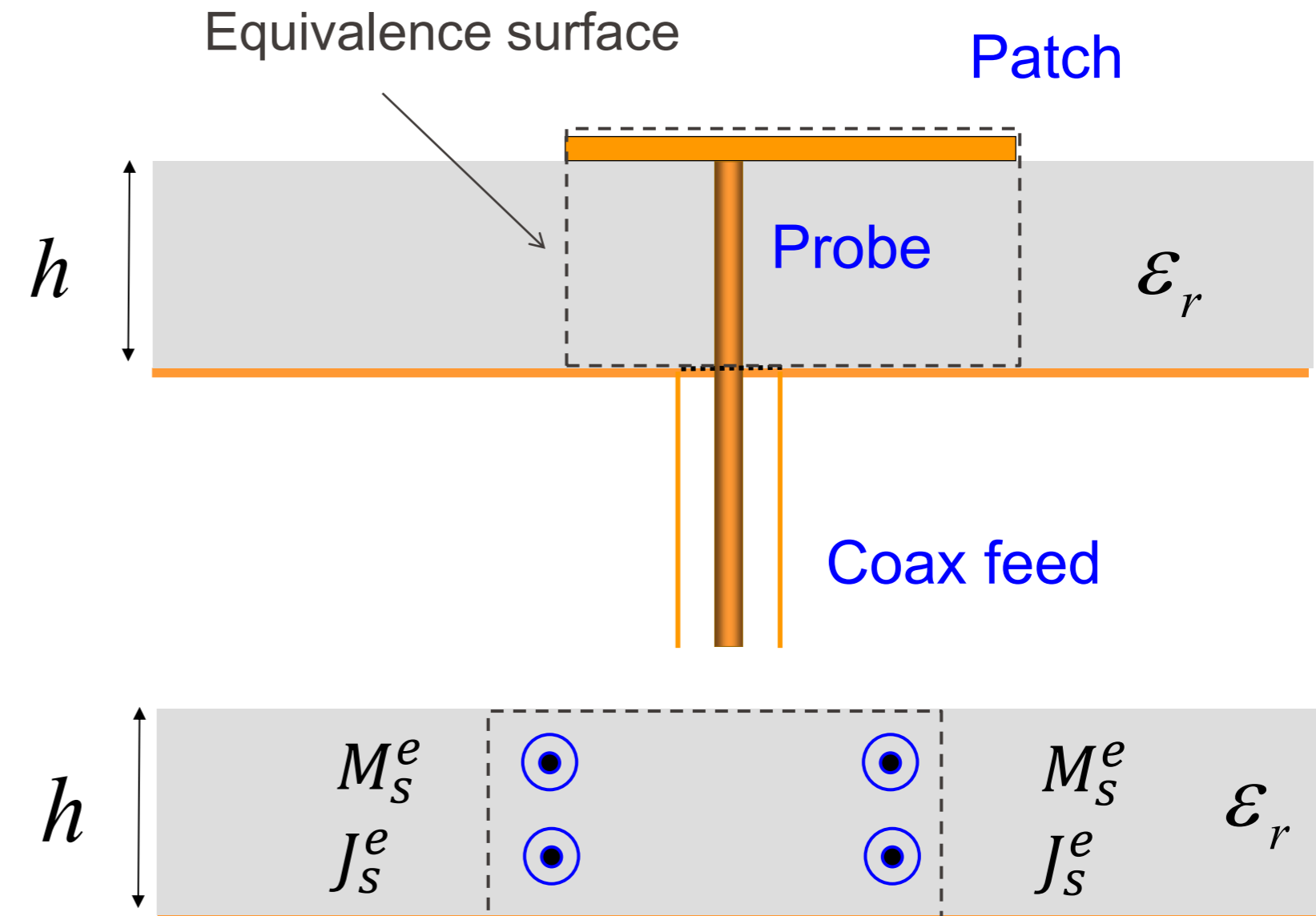
$$f_{020} = \frac{1}{2\sqrt{\mu\epsilon}} \left(\frac{2}{W} \right) = \frac{v_0}{\sqrt{\epsilon_r}} \left(\frac{1}{L} \right)$$

Field configurations (**modes**) for rectangular microstrip patch. In all of the preceding discussion, it was assumed that there is no fringing of the fields along the edges of the cavity. This is not totally valid, but it is a good assumption. However, fringing effects and their influence were discussed previously, and they should be taken into account in determining the resonant frequency.

Using the Field Equivalence Principle (*Huygens' Principle*), the microstrip patch is represented by an equivalent electric current density \mathbf{J}_t at the top surface of the patch to account for the presence of the patch (there is also a current density \mathbf{J}_b at the bottom of the patch which is not needed for this model). The four side slots are represented by the equivalent electric current density \mathbf{J}_s^e and equivalent magnetic current density \mathbf{M}_s^e , as shown in the following figure, each represented by

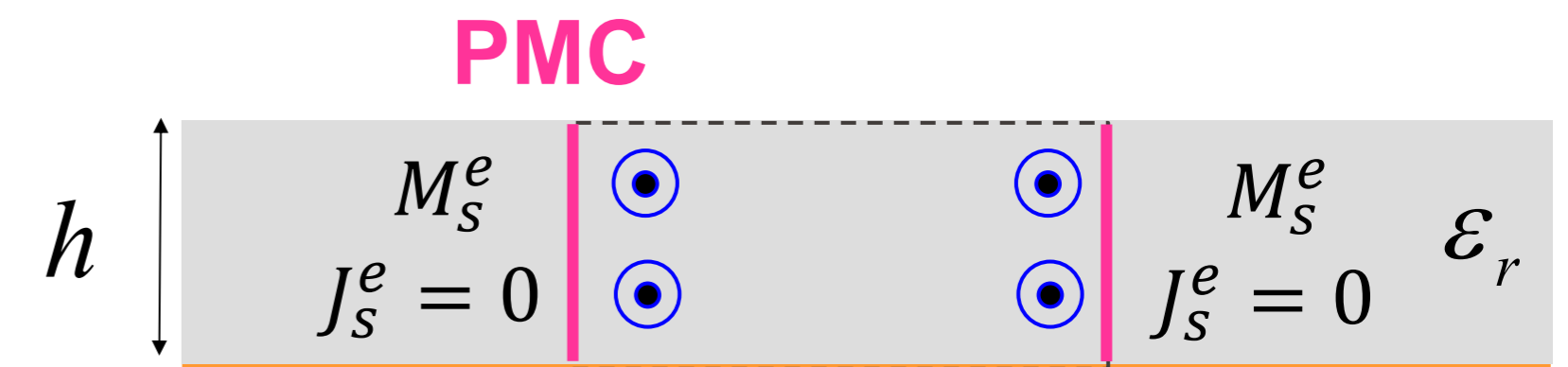
$$\vec{M}_s^e = -\hat{n} \times \vec{E} \quad \vec{J}_s^e = \hat{n} \times \vec{H}$$

where \mathbf{E} and \mathbf{H} represent, respectively, the electric and magnetic fields at the slots.



It has been shown using the cavity model that the microstrip antenna can be modeled reasonably well by a dielectric-loaded cavity with two perfectly conducting electric (**PEC**) walls (top and bottom), and four perfectly conducting magnetic (**PMC**) walls (sidewalls). It is assumed that the material of the substrate is truncated and does not extend beyond the edges of the patch.

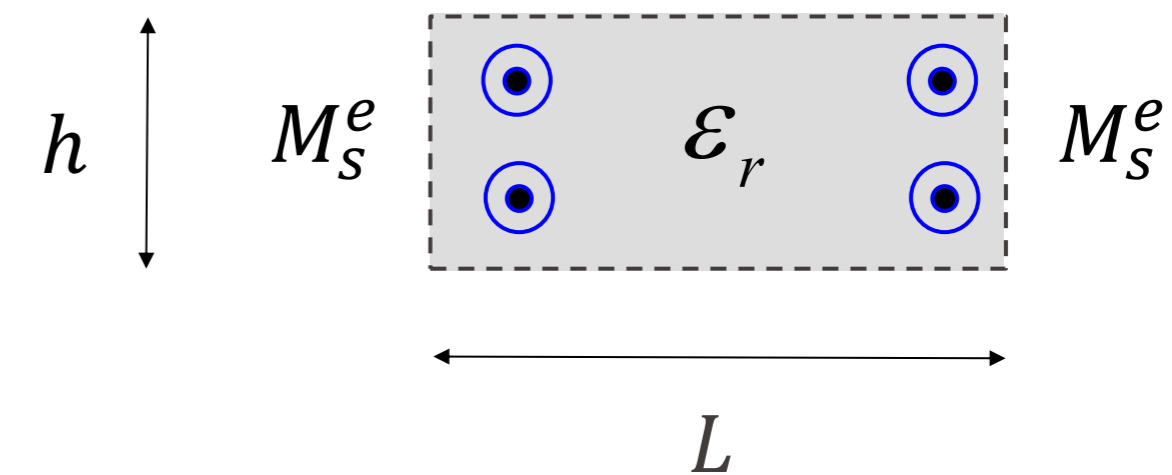
$$\vec{J}_s^e = \hat{n} \times \vec{H} \approx 0$$



Thus the only nonzero current density is the equivalent magnetic current density \mathbf{M}_s along the side periphery of the cavity radiating in the presence of the ground plane, as shown in the figure.

The presence of the ground plane can be taken into account by **image theory** which will double the equivalent magnetic current density of \mathbf{M}_s . Therefore the final equivalent is a magnetic current density of twice \mathbf{M}_s or

$$\overline{\mathbf{M}}_s^e = -2\hat{n} \times \vec{E}$$



Cavity Model

Equivalent Current Densities

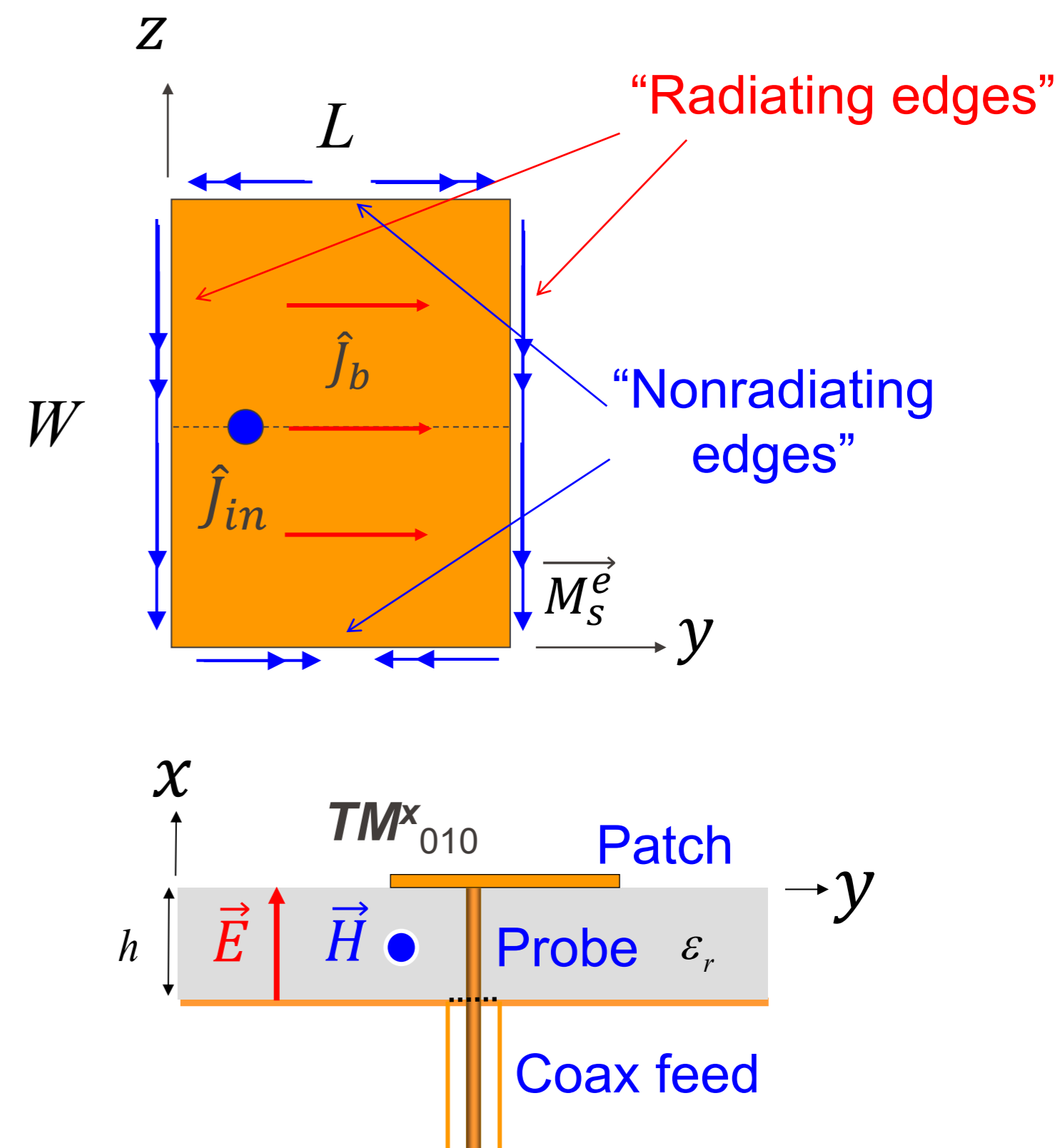
Assuming that the dominant mode within the cavity is the TM^x_{010} mode, the electric and magnetic field components reduce from

$$\hat{J}_{in} = A^J_{010} \cos\left(\frac{\pi y'}{L}\right) \xrightarrow{TM^x_{010}} A_x(y')$$

$$\vec{H}_A = \frac{1}{\mu} \nabla \times A \xrightarrow{} -\hat{z} \frac{\partial A_x(y')}{\partial y'} = \hat{z} \sin\left(\frac{\pi y'}{L}\right) = H_z$$

$$\vec{E}_A = \frac{1}{j\omega\epsilon} \nabla \times \vec{H}_A \xrightarrow{} \hat{x} \frac{\partial}{\partial y'} \left[\sin\left(\frac{\pi y'}{L}\right) \right] = \hat{x} \cos\left(\frac{\pi y'}{L}\right) = E_x$$

Antennas



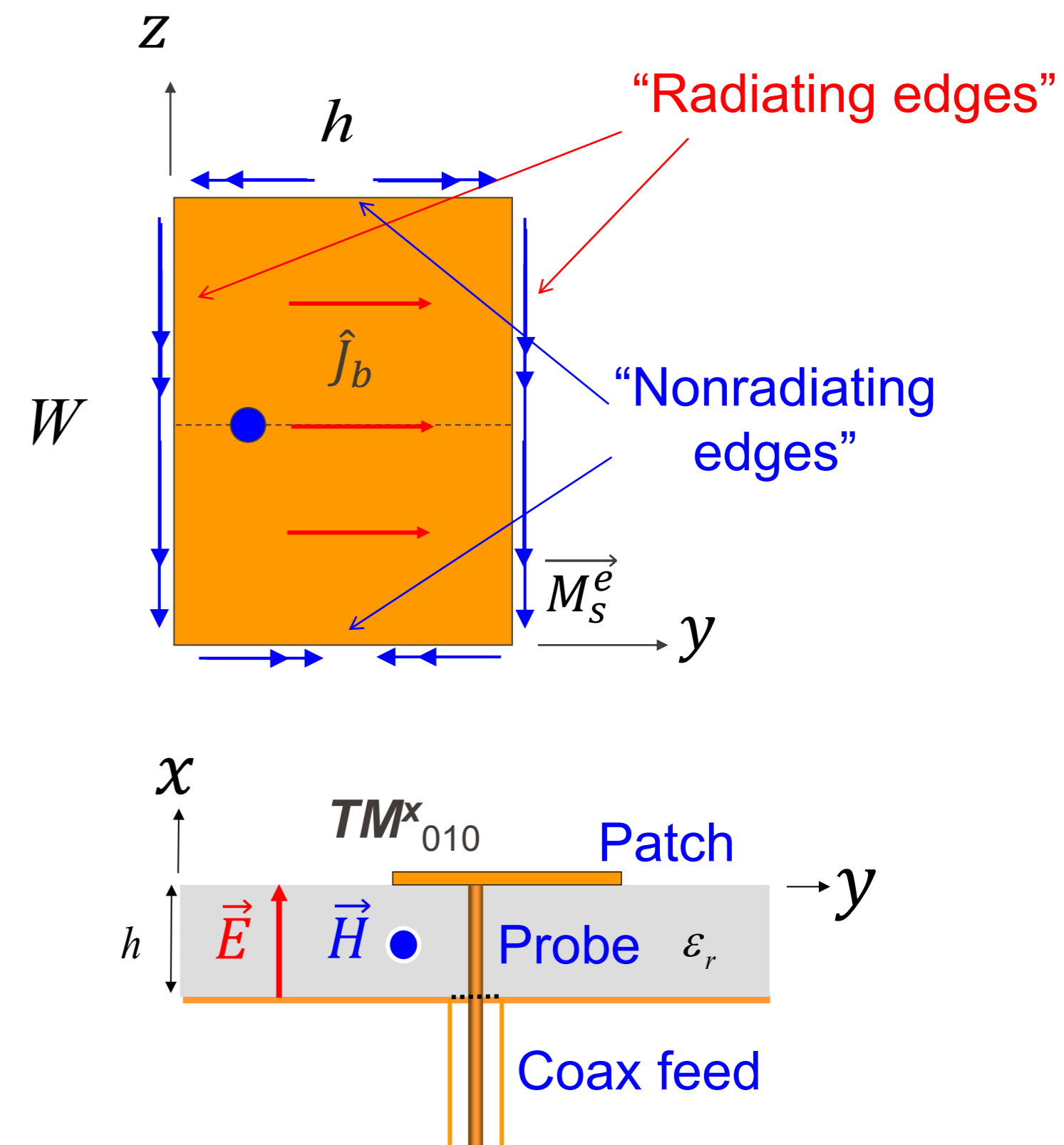
While there are a total of four slots representing the microstrip antenna, only two (the radiating slots) account for most of the radiation; the fields radiated by the other two, which are separated by the width W of the patch, cancel along the principal planes. Therefore the same two slots, separated by the length of the patch, are referred to here as radiating slots.

$$E_x = E_0 \cos\left(\frac{\pi}{L}y'\right)$$

$$H_z = H_0 \sin\left(\frac{\pi}{L}y'\right)$$

$$E_y = E_z = H_x = H_y = 0$$

where $E_0 = -j\omega A_{010}$ and $H_0 = (\pi/\mu L)A_{010}$.



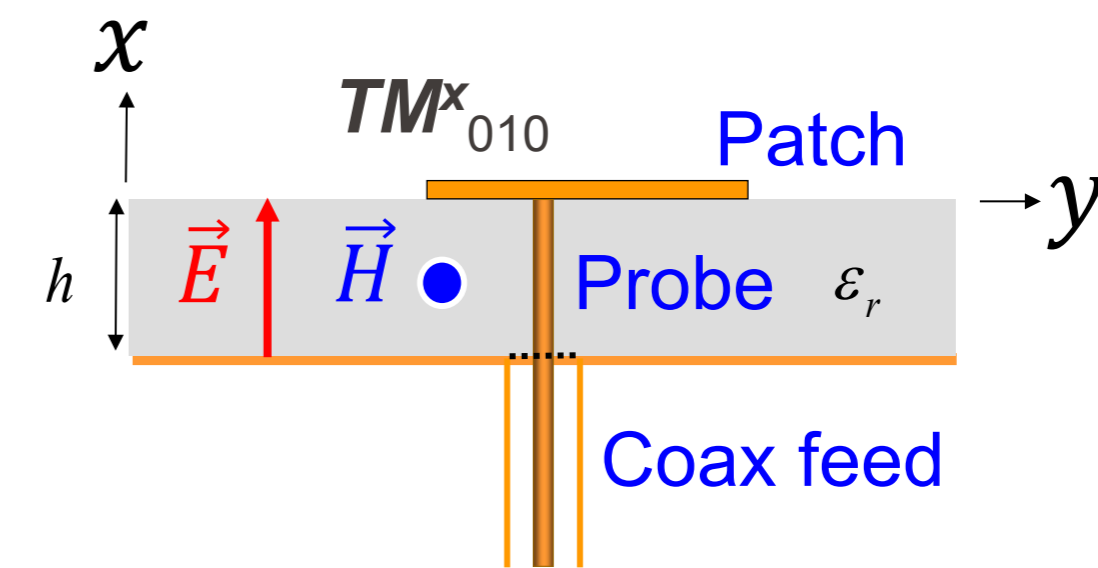
On the nonradiating edges, the magnetic currents are in opposite directions across the centerline ($y = 0$).

$$E_x = E_0 \cos\left(\frac{\pi}{L}y'\right)$$

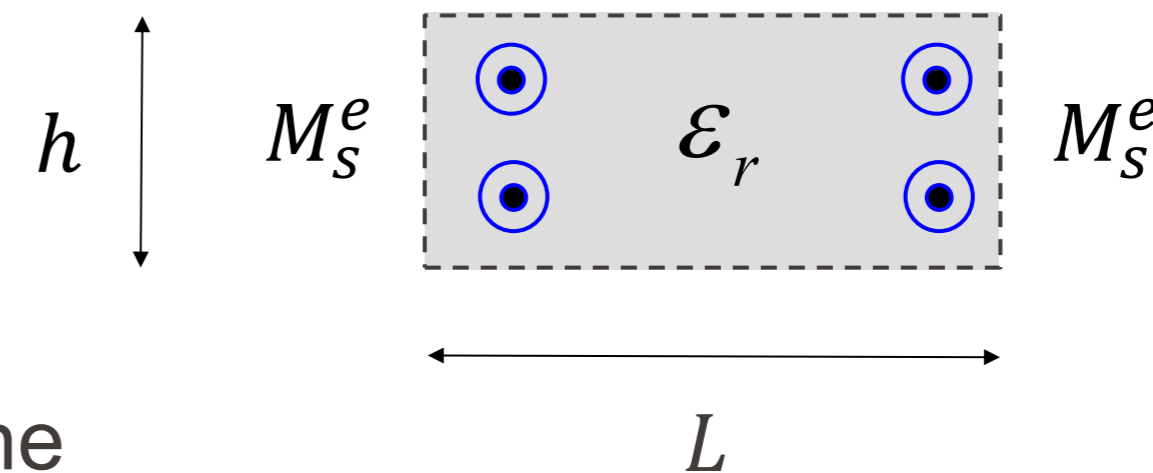
$$H_z = H_0 \sin\left(\frac{\pi}{L}y'\right)$$

$$E_y = E_z = H_x = H_y = 0$$

where $E_0 = -j\omega A_{010}$ and $H_0 = (\pi/\mu L)A_{010}$.



$$\vec{M}_s^e = -2\hat{n} \times \vec{E}_x$$



In the magnetic current model, the magnetic currents on the nonradiating edges do not contribute to the \mathbf{E} and \mathbf{H} plane patterns.

EPFL Cavity Model

Recall: Vector Potential

Electric and Magnetic Fields for Electric, \mathbf{J} , and Magnetic, \mathbf{M} , Current Sources: The procedure requires that the auxiliary potential functions \mathbf{A} and \mathbf{F} generated, respectively, by \mathbf{J} and \mathbf{M} are found first.

$$\mathbf{A} = \frac{\mu}{4\pi} \iiint_V \mathbf{J} \frac{e^{-jkR}}{R} dv'$$

$$\mathbf{F} = \frac{\epsilon}{4\pi} \iiint_V \mathbf{M} \frac{e^{-jkR}}{R} dv'$$

TABLE 3.1 Dual Equations for Electric (\mathbf{J}) and Magnetic (\mathbf{M}) Current Sources

Electric Sources
($\mathbf{J} \neq 0, \mathbf{M} = 0$)

Magnetic Sources
($\mathbf{J} = 0, \mathbf{M} \neq 0$)

$$\nabla \times \mathbf{E}_A = -j\omega\mu\mathbf{H}_A$$

$$\nabla \times \mathbf{H}_F = j\omega\epsilon\mathbf{E}_F$$

$$\nabla \times \mathbf{H}_A = \mathbf{J} + j\omega\epsilon\mathbf{E}_A$$

$$-\nabla \times \mathbf{E}_F = \mathbf{M} + j\omega\mu\mathbf{H}_F$$

$$\nabla^2 \mathbf{A} + k^2 \mathbf{A} = -\mu\mathbf{J}$$

$$\nabla^2 \mathbf{F} + k^2 \mathbf{F} = -\epsilon\mathbf{M}$$

$$\mathbf{A} = \frac{\mu}{4\pi} \iiint_V \mathbf{J} \frac{e^{-jkR}}{R} dv'$$

$$\mathbf{F} = \frac{\epsilon}{4\pi} \iiint_V \mathbf{M} \frac{e^{-jkR}}{R} dv'$$

$$\mathbf{H}_A = \frac{1}{\mu} \nabla \times \mathbf{A}$$

$$\mathbf{E}_F = -\frac{1}{\epsilon} \nabla \times \mathbf{F}$$

$$\mathbf{E}_A = -j\omega\mathbf{A} - j\frac{1}{\omega\mu\epsilon} \nabla(\nabla \cdot \mathbf{A})$$

$$\mathbf{H}_F = -j\omega\mathbf{F} - j\frac{1}{\omega\mu\epsilon} \nabla(\nabla \cdot \mathbf{F})$$

Recall: Vector Potential & Far-field Radiation

$$\mathbf{F} = \frac{\epsilon}{4\pi} \iint_S \mathbf{M}_s \frac{e^{-jkR}}{R} ds' \simeq \frac{\epsilon e^{-jkr}}{4\pi r} \mathbf{L}$$

$$\mathbf{L} = \iint_S \mathbf{M}_s e^{jkr' \cos \psi} ds'$$

$$\mathbf{A} = \frac{\mu}{4\pi} \iint_S \mathbf{J}_s \frac{e^{-jkR}}{R} ds' \simeq \frac{\mu e^{-jkr}}{4\pi r} \mathbf{N}$$

$$\mathbf{N} = \iint_S \mathbf{J}_s e^{jkr' \cos \psi} ds'$$

Recall: Vector Potential & Far-field Radiation

Since

$$\begin{aligned} \vec{M}_s^e &= -2\hat{n} \times \vec{E}_x \longrightarrow \vec{M}_z^e \\ \vec{J}_s^e &= \hat{n} \times \vec{H} \approx 0 \longrightarrow \mathbf{N} = 0 \end{aligned}$$

Thus

$$L_\theta = \iint_S [\cancel{M_x} \cos \theta \cos \phi + \cancel{M_y} \cos \theta \sin \phi - M_z \sin \theta] e^{+jkr' \cos \psi} ds'$$

$$L_\phi = \iint_S [-\cancel{M_x} \sin \phi + \cancel{M_y} \cos \phi] e^{+jkr' \cos \psi} ds' = 0$$

Recall: Vector Potential & Far-field Radiation

$$E_r \simeq 0$$

$$E_\theta \simeq -\frac{jke^{-jkr}}{4\pi r} (\cancel{L_\phi} + \eta \cancel{M_\theta})$$

$$E_\phi \simeq +\frac{jke^{-jkr}}{4\pi r} (L_\theta - \eta \cancel{M_\phi})$$

$$H_r \simeq 0$$

$$H_\theta \simeq \frac{jke^{-jkr}}{4\pi r} \left(\cancel{M_\theta} - \frac{L_\theta}{\eta} \right)$$

$$H_\phi \simeq -\frac{jke^{-jkr}}{4\pi r} \left(\cancel{M_\phi} + \frac{\cancel{L_\phi}}{\eta} \right)$$

→

$$E_r \simeq E_\theta \simeq 0$$

$$E_\phi = +j \frac{k_0 h W E_0 e^{-jk_0 r}}{2\pi r} \left\{ \sin \theta \frac{\sin(X)}{X} \frac{\sin(Z)}{Z} \right\}$$

$$X = \frac{k_0 h}{2} \sin \theta \cos \phi$$

$$Z = \frac{k_0 W}{2} \cos \theta$$

The array factor for the two elements, of the same magnitude and phase, separated by a distance L_e along the y direction is

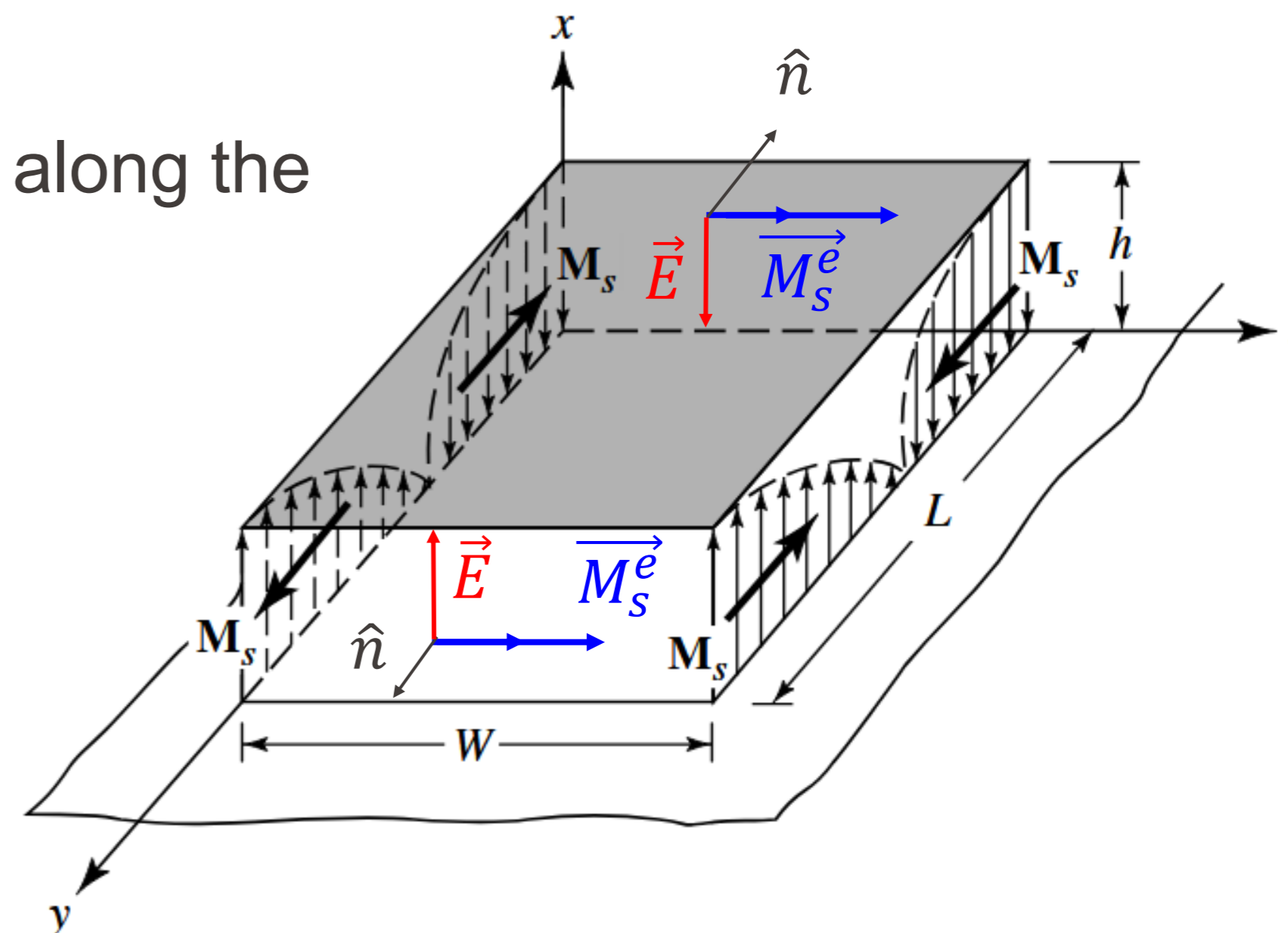
$$(AF)_y = 2 \cos \left(\frac{k_0 L_e}{2} \sin \theta \sin \phi \right)$$

where L_e is the effective length of a patch. Thus, the total electric field for the two slots (also for the microstrip antenna) is

$$E_\phi^t = +j \frac{k_0 h W E_0 e^{-jk_0 r}}{\pi r} \left\{ \sin \theta \frac{\sin(X)}{X} \frac{\sin(Z)}{Z} \right\} \times \cos \left(\frac{k_0 L_e}{2} \sin \theta \sin \phi \right)$$

single slot

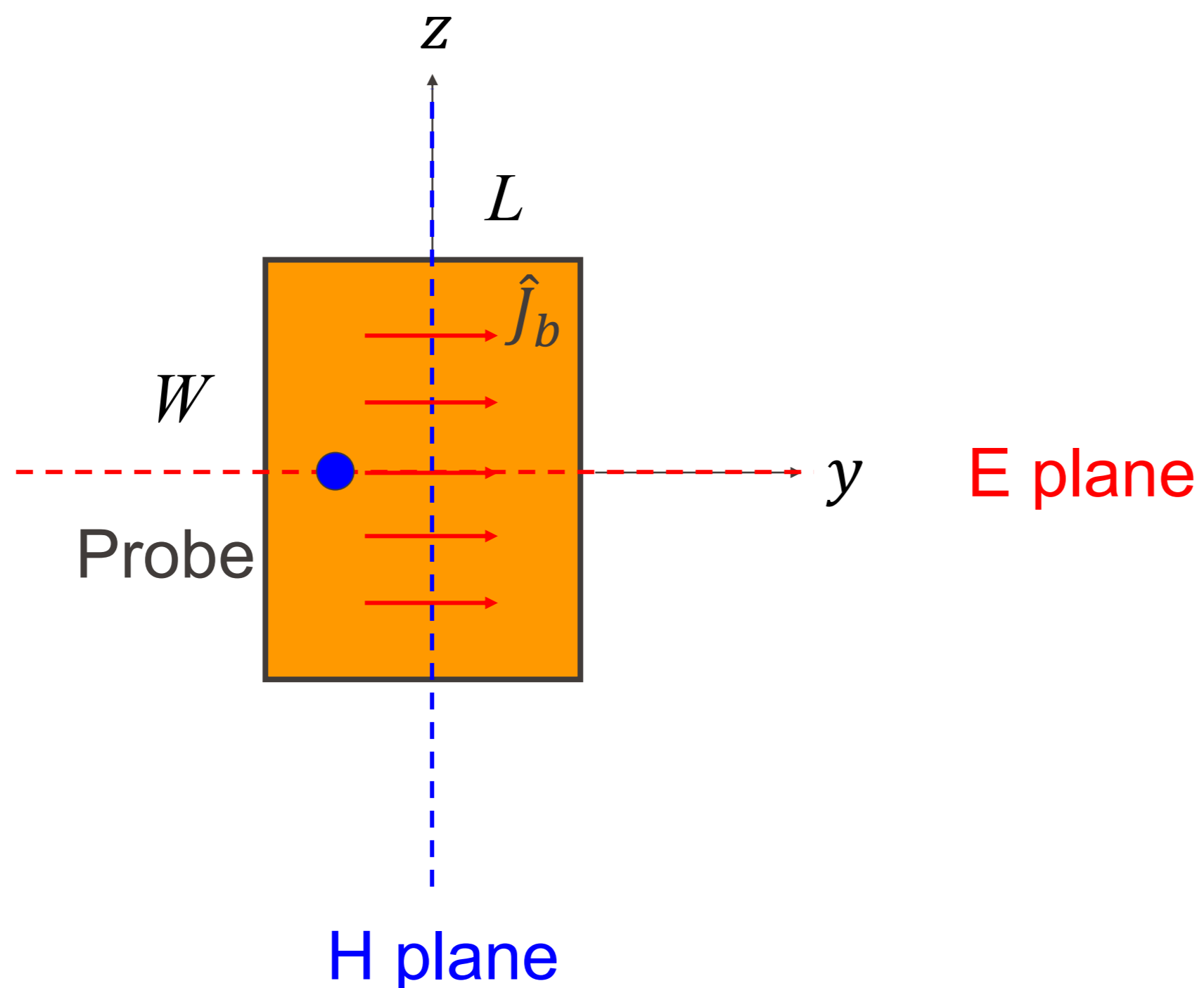
array factor



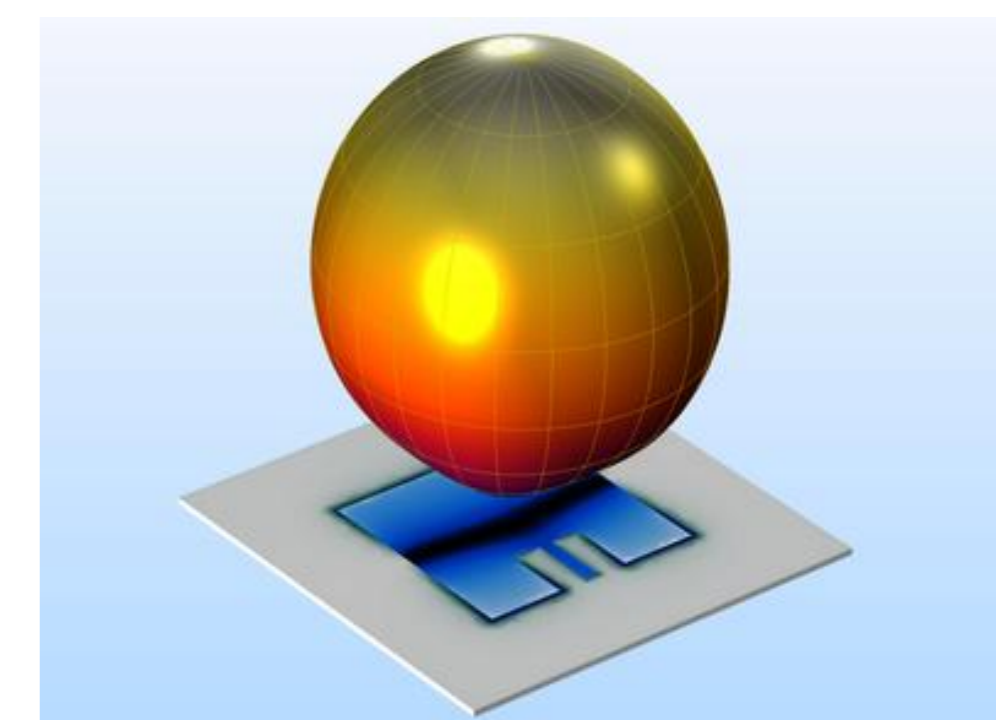
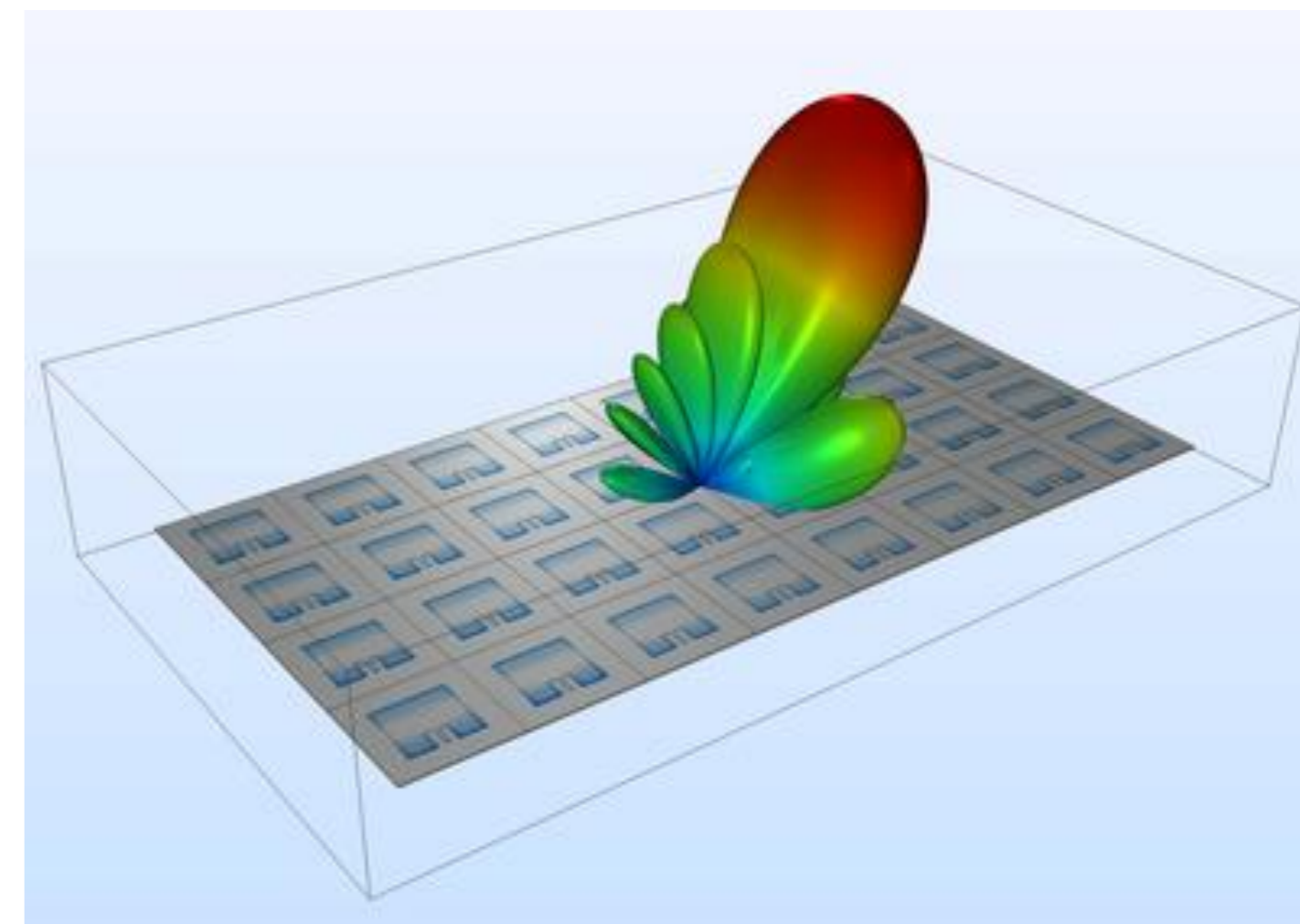
Cavity Model

Radiation Pattern

Recall: An E-plane is a plane within an electromagnetic wave that contains the electric field vector and the **direction of maximum radiation from an antenna**, dictating the polarization of the wave.



Antennas



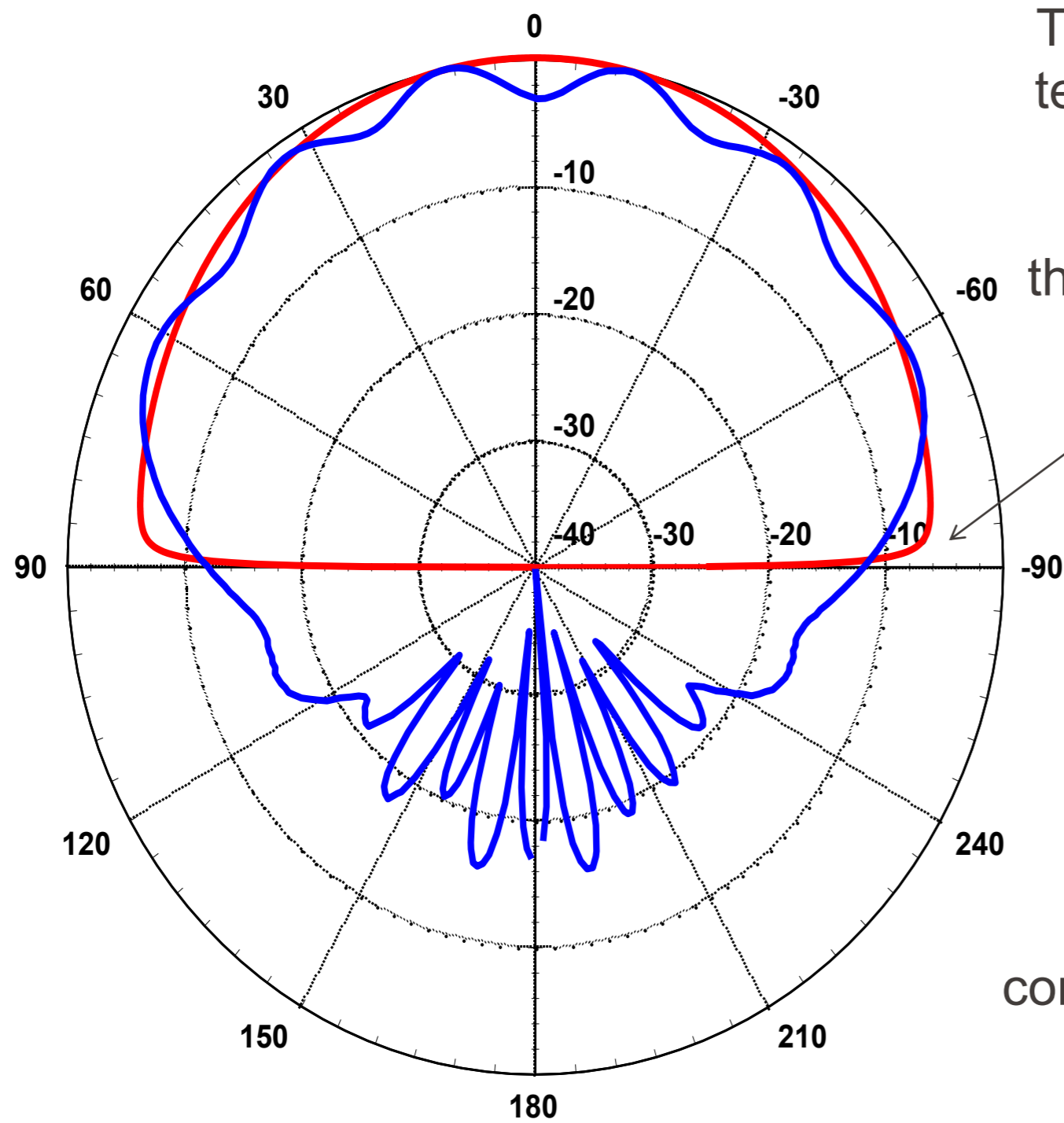
Edge diffraction is the most serious in the E plane.

Cavity Model

Radiation Pattern

Red: infinite substrate and ground plane

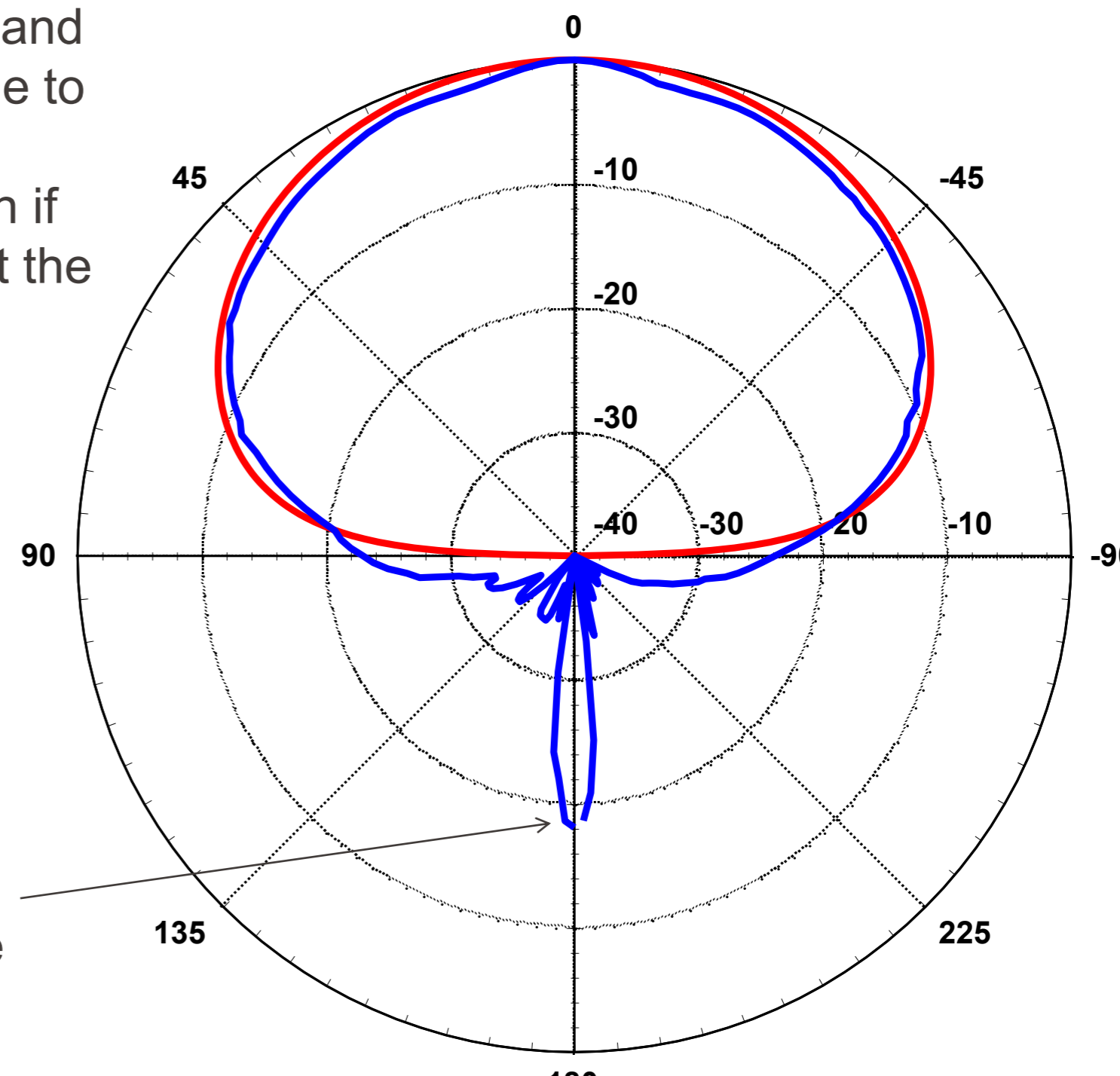
Blue: 1 meter ground plane



E-plane pattern

The E-plane pattern “tucks in” and tends to zero at the horizon due to the presence of the infinite substrate. (It would not tuck in if the substrate were truncated at the patch edges.)

E-plane diffraction only contributes to the H-plane in the back boresight direction.



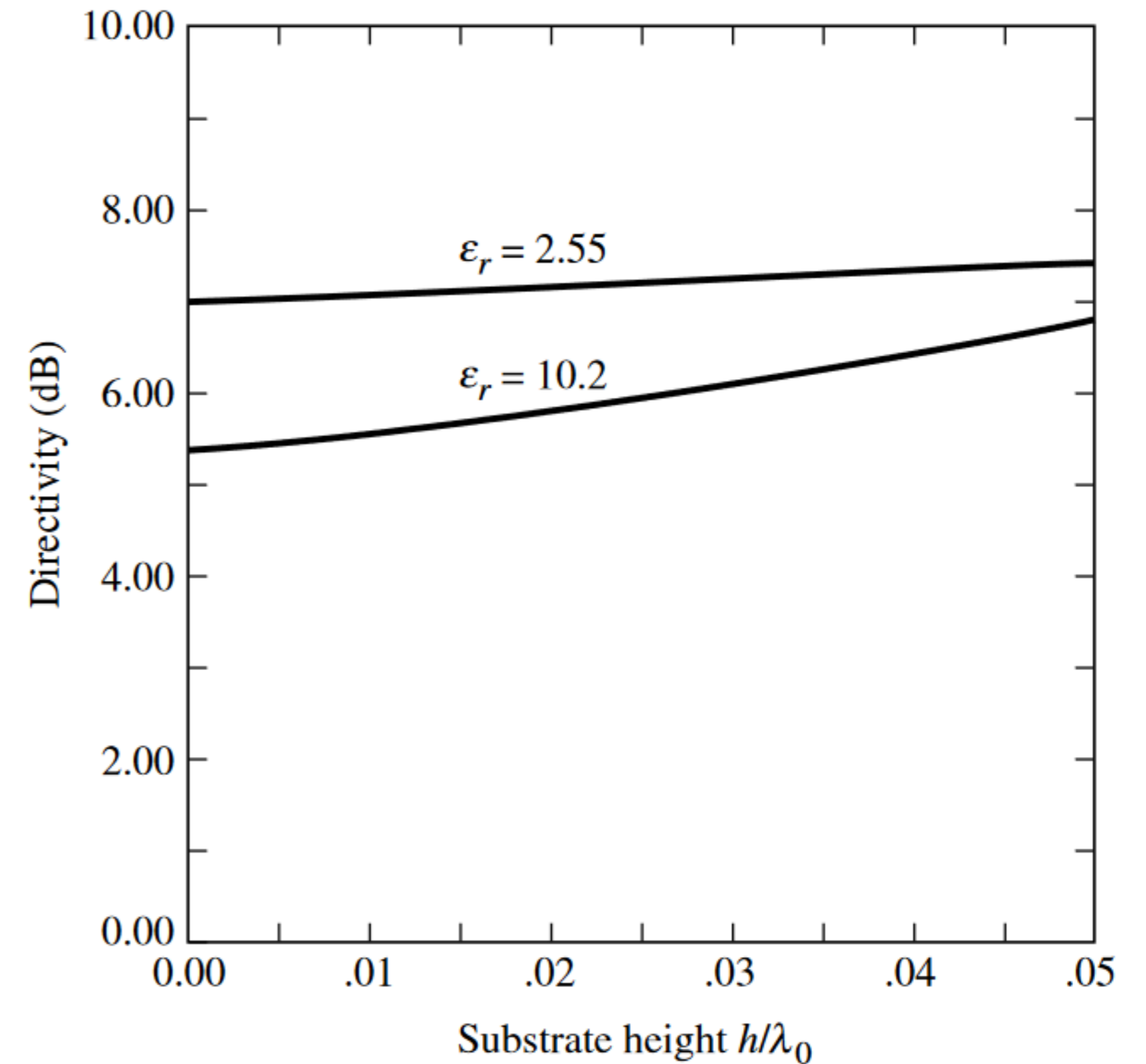
H-plane pattern

Antennas

Asymptotically the directivity of two slots (microstrip antenna) can be expressed as

$$D_2 = \begin{cases} 6.6(\text{dimensionless}) = 8.2 \text{ dB} & W \ll \lambda_0 \\ 8 \left(\frac{W}{\lambda_0} \right) & W \gg \lambda_0 \end{cases}$$

Directivity variations as a function of substrate height for a square microstrip patch antenna.



Input Impedance

The patch is usually fed along the centerline ($z_0 = W / 2$)

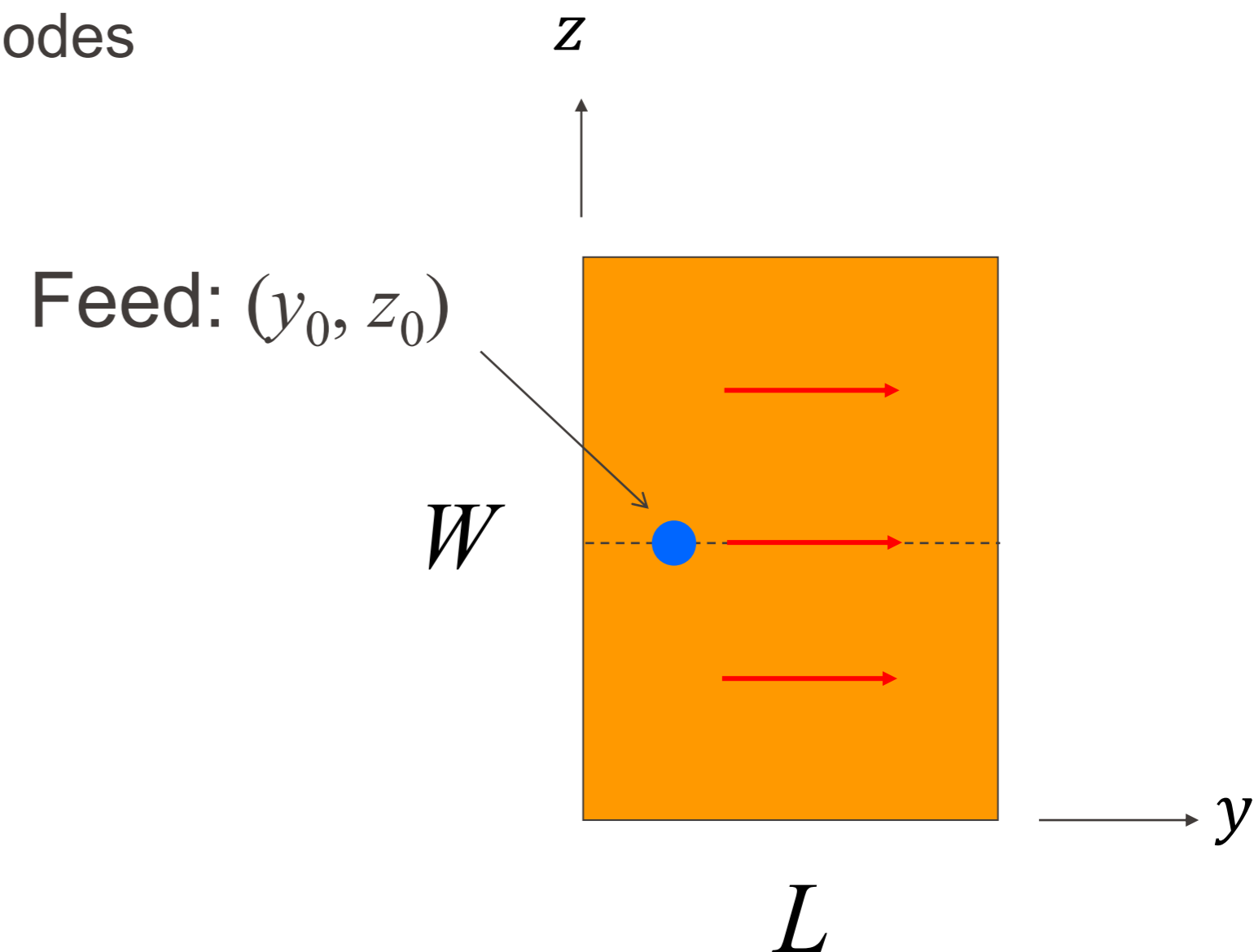
To maintain symmetry and thus minimize excitation of undesirable modes (which cause cross-pol), when the desired mode is (0,1,0),

The TM_{001} mode is not excited for a feed on the centerline.

$$E_x^{(1,0)} = \cos\left(\frac{\pi y}{L}\right)$$

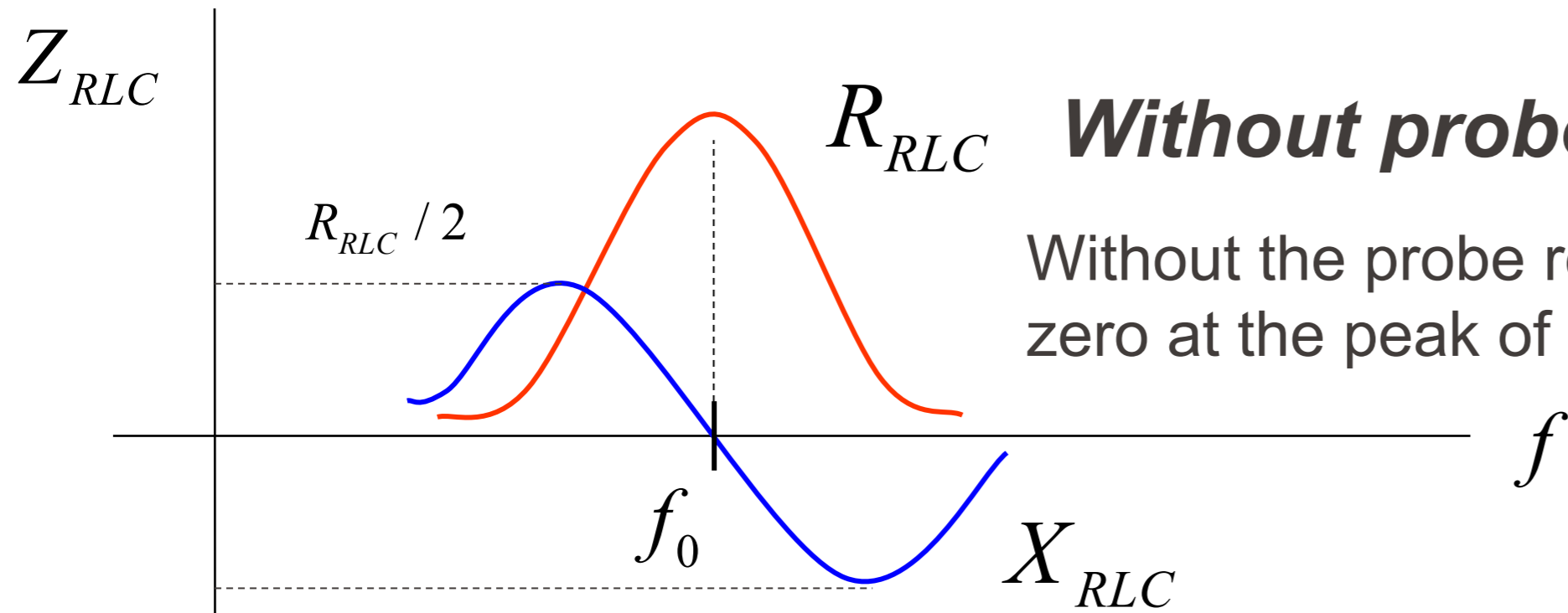
$$E_x^{(0,1)} = \cos\left(\frac{\pi z}{W}\right) \quad (\text{zero on centerline})$$

$$R_{\text{in}} \propto E_x^2(y_0, z_0) \quad \rightarrow \quad R_{\text{in}} \propto \cos^2\left(\frac{\pi y_0}{L}\right)$$



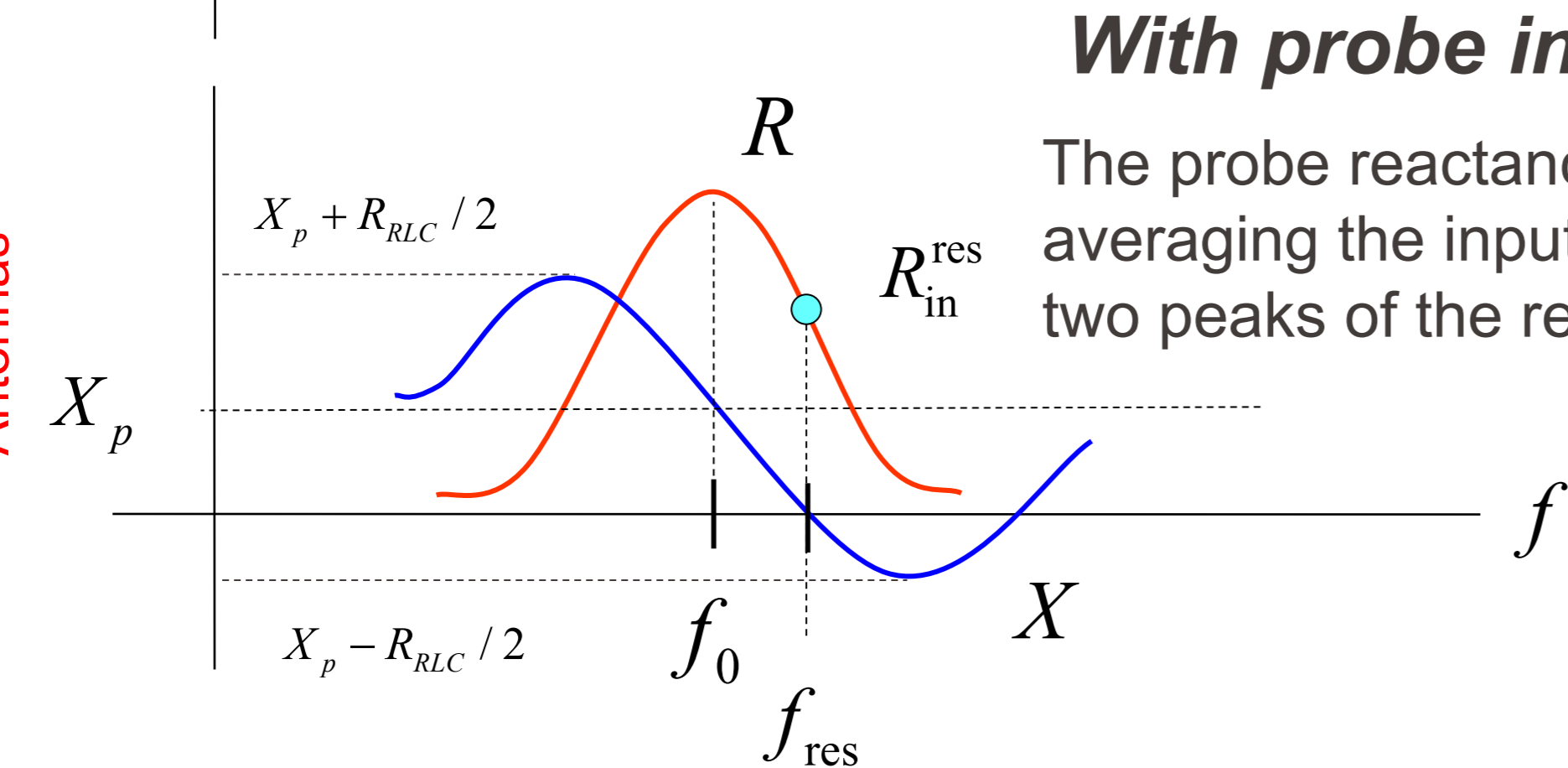
For a given mode, it can be shown that the resonant input resistance is proportional to the square of the cavity-mode field at the feed point.

Input Impedance



Without probe inductance

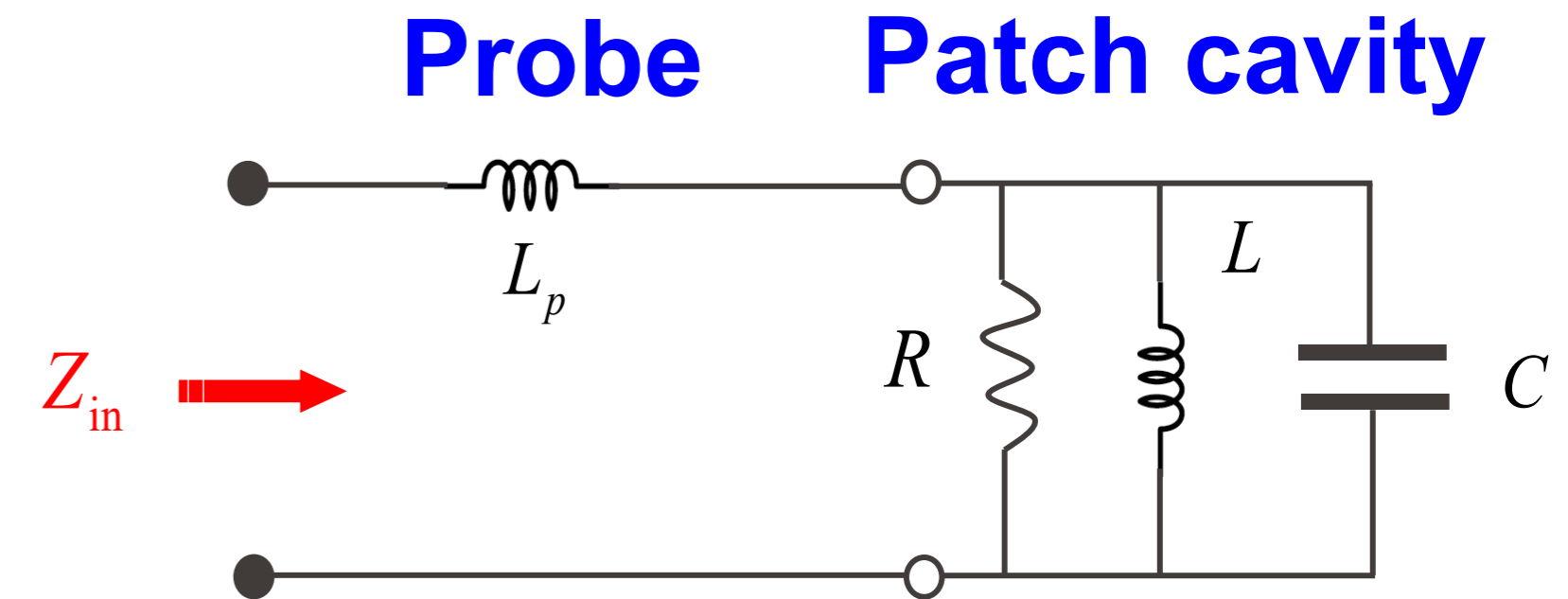
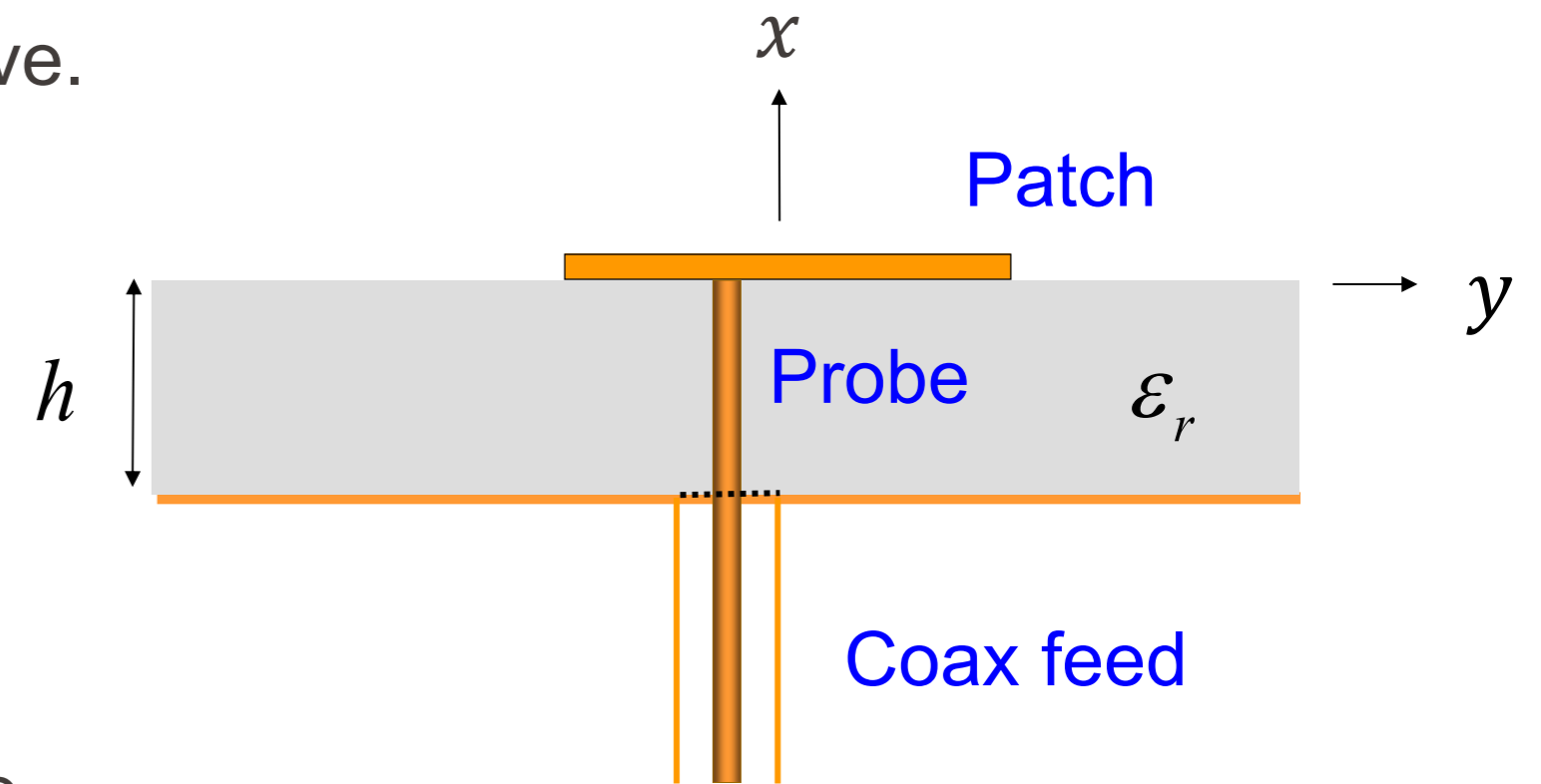
Without the probe reactance, the input reactance is zero at the peak of the input resistance curve.



With probe inductance

The probe reactance can be found by averaging the input reactance values at the two peaks of the reactance curve.

Antennas



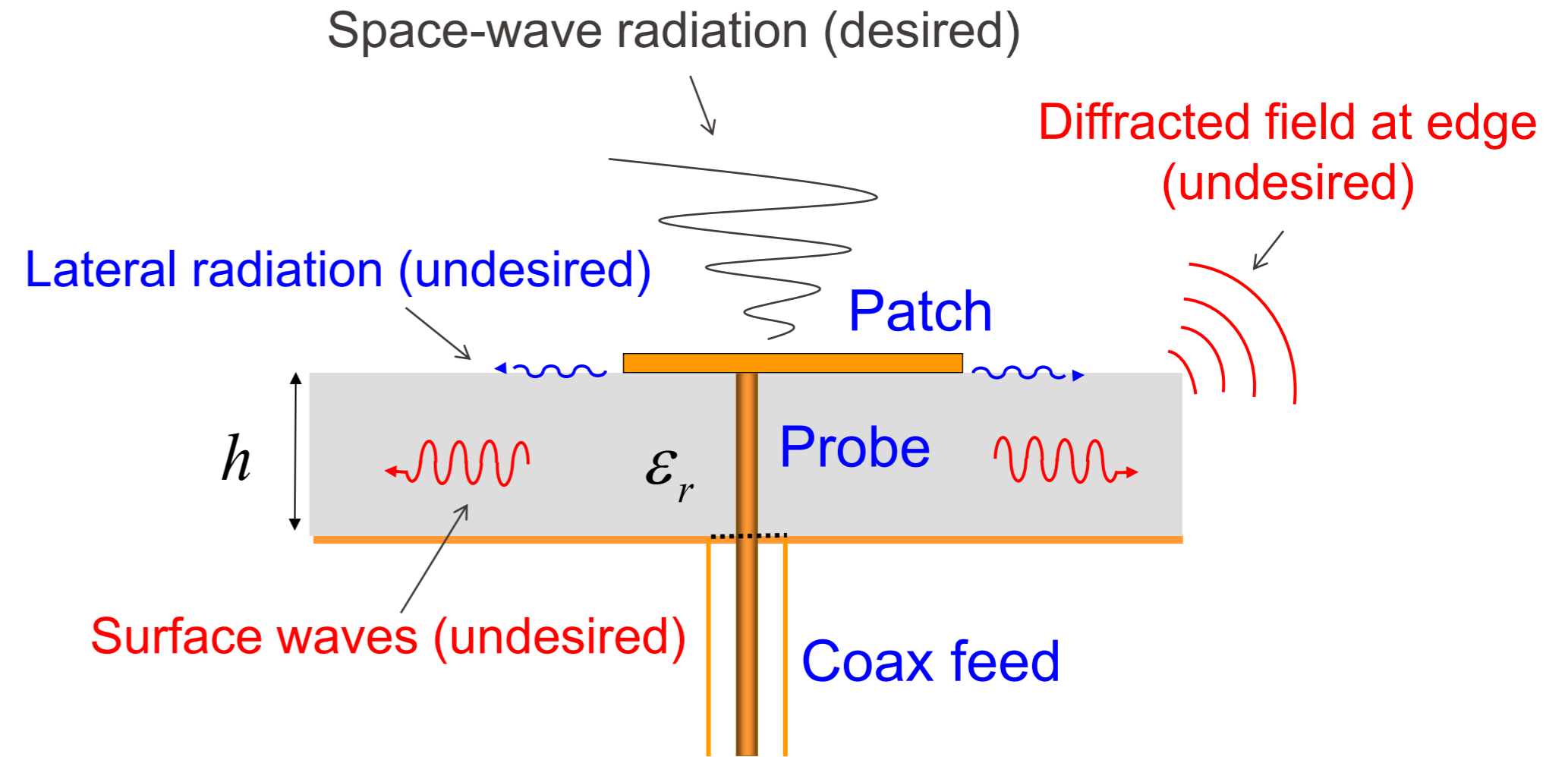
Quality Factor, Bandwidth, and Efficiency

The quality factor is a figure-of-merit that is representative of the antenna losses. Typically there are radiation, conduction (ohmic), dielectric and surface wave losses. Therefore the total quality factor Q_t is influenced by all of these losses and is, in general, written as

- Q_t = total quality factor
- Q_{rad} = quality factor due to radiation(space wave) losses
- Q_c = quality factor due to conduction (ohmic) losses
- Q_d = quality factor due to dielectric losses
- Q_{sw} = quality factor due to surface waves

Antennas

For very thin substrates, the losses due to surface waves are very small and can be neglected. However, for thicker substrates they need to be taken into account.



$$Q_{rad} = \frac{2\omega\epsilon_r}{hG_t/l} K$$

$$Q_c = h\sqrt{\pi f \mu \sigma}$$

$$Q_d = \frac{1}{\tan \delta}$$

$$\frac{1}{Q_t} = \frac{1}{Q_{rad}} + \frac{1}{Q_c} + \frac{1}{Q_d} + \frac{1}{Q_{sw}}$$

For a rectangular aperture operating in the dominant TM^x_{010} mode

$$K = \frac{L}{4}$$

$$G_t/l = \frac{G_{rad}}{W}$$

where $\tan \delta$ is the loss tangent of the substrate material, σ is the conductivity of the conductors associated with the patch and ground plane, G_t/l is the total conductance per unit length of the radiating aperture.

Quality Factor, Bandwidth, and Efficiency

The fractional bandwidth of the antenna is inversely proportional to the Q_t of the antenna, and it is defined by

$$\frac{\Delta f}{f_0} = \frac{1}{Q_t}$$

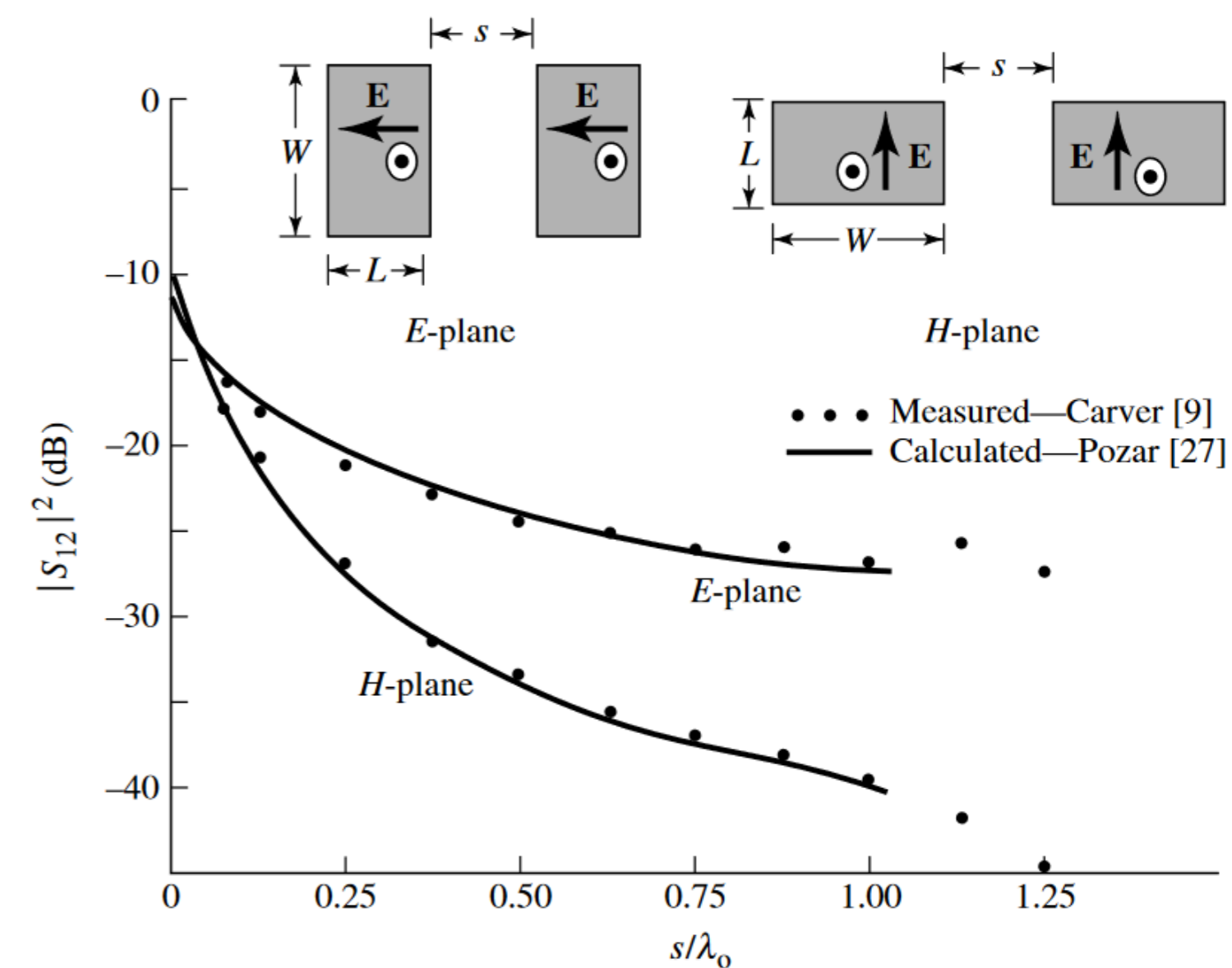
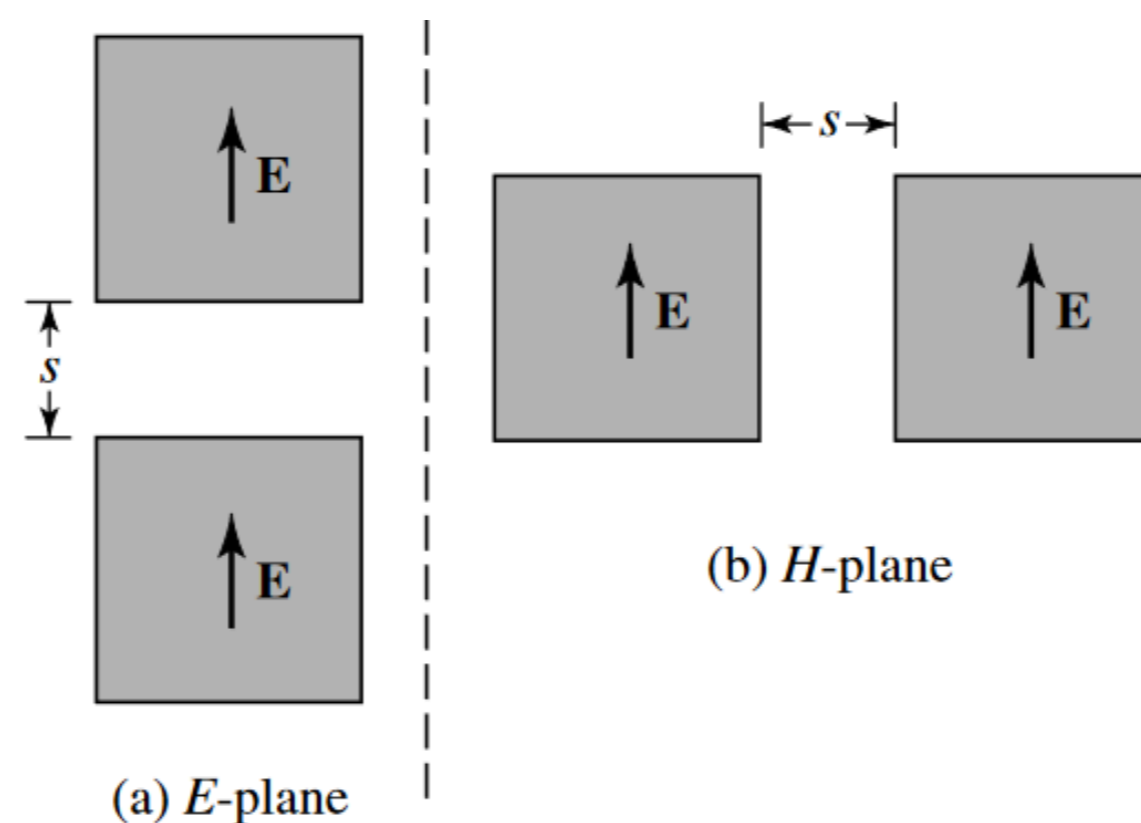
However, this may not be as useful because it does not take into account *impedance matching* at the input terminals of the antenna. A more meaningful definition of the fractional bandwidth is over a band of frequencies where the VSWR at the input terminals is equal to or less than a desired maximum value, assuming that the VSWR is unity at the design frequency. A modified form of this equation that takes into account the impedance matching is

$$\frac{\Delta f}{f_0} = \frac{\text{VSWR} - 1}{Q_t \sqrt{\text{VSWR}}}$$

Mutual Coupling

The coupling between two or more microstrip antenna elements can be taken into account easily using full-wave analysis. For two rectangular microstrip patches the coupling for two side-by-side elements is a function of the relative alignment. When the elements are positioned collinearly along the E-plane, this arrangement is referred to as the E-plane; when the elements are positioned collinearly along the H-plane, this arrangement is referred to as the H-plane.

For an edge-to-edge separation of s , the E-plane exhibits the smallest coupling isolation for very small spacing (typically $s < 0.10\lambda_0$) while the H-plane exhibits the smallest coupling for large spacing (typically $s > 0.10\lambda_0$). The spacing at which one plane coupling overtakes the other one depends on the electrical properties and geometrical dimensions of the microstrip antenna.

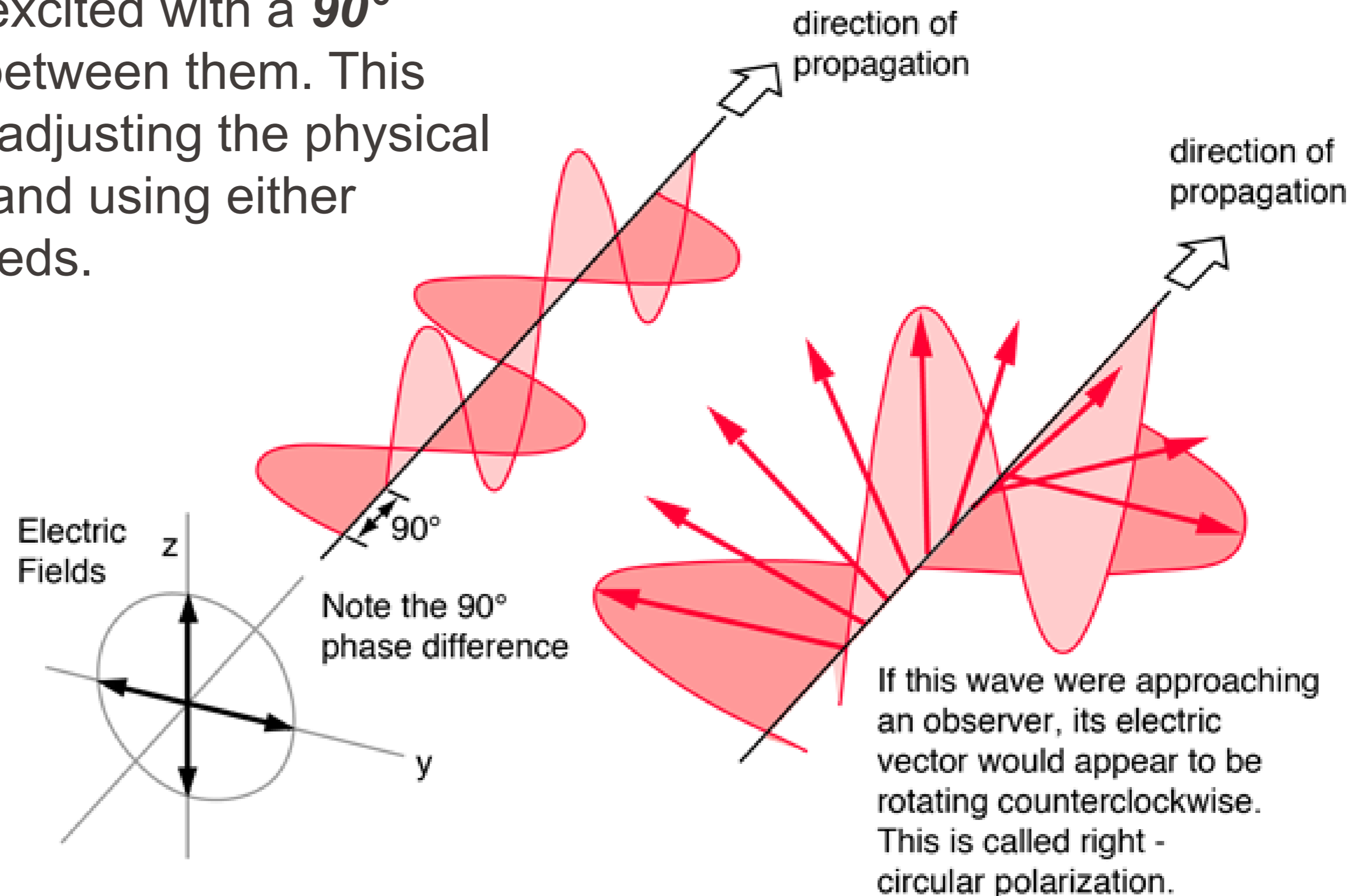


In general, mutual coupling is primarily attributed to the fields that exist along the air-dielectric interface. In a given direction, the lowest order (dominant) surface wave mode is TM with zero cutoff frequency followed by a TE, and alternatively by TM and TE modes. For a rectangular microstrip patch, the fields are TM in a direction of propagation along the E-plane and TE in a direction of propagation along the H-plane.

Since for the E-plane arrangement, the elements are placed collinearly along the E-plane where the fields in the space between the elements are primarily TM, there is a stronger surface wave excitation (based on a single dominant surface wave mode) between the elements, and the coupling is larger. However for the H-plane arrangement, the fields in the space between the elements are primarily TE and there is not a strong dominant mode surface wave excitation; therefore there is less coupling between the elements. This does change as the thickness of the substrate increases which allows higher order TE surface wave excitation.

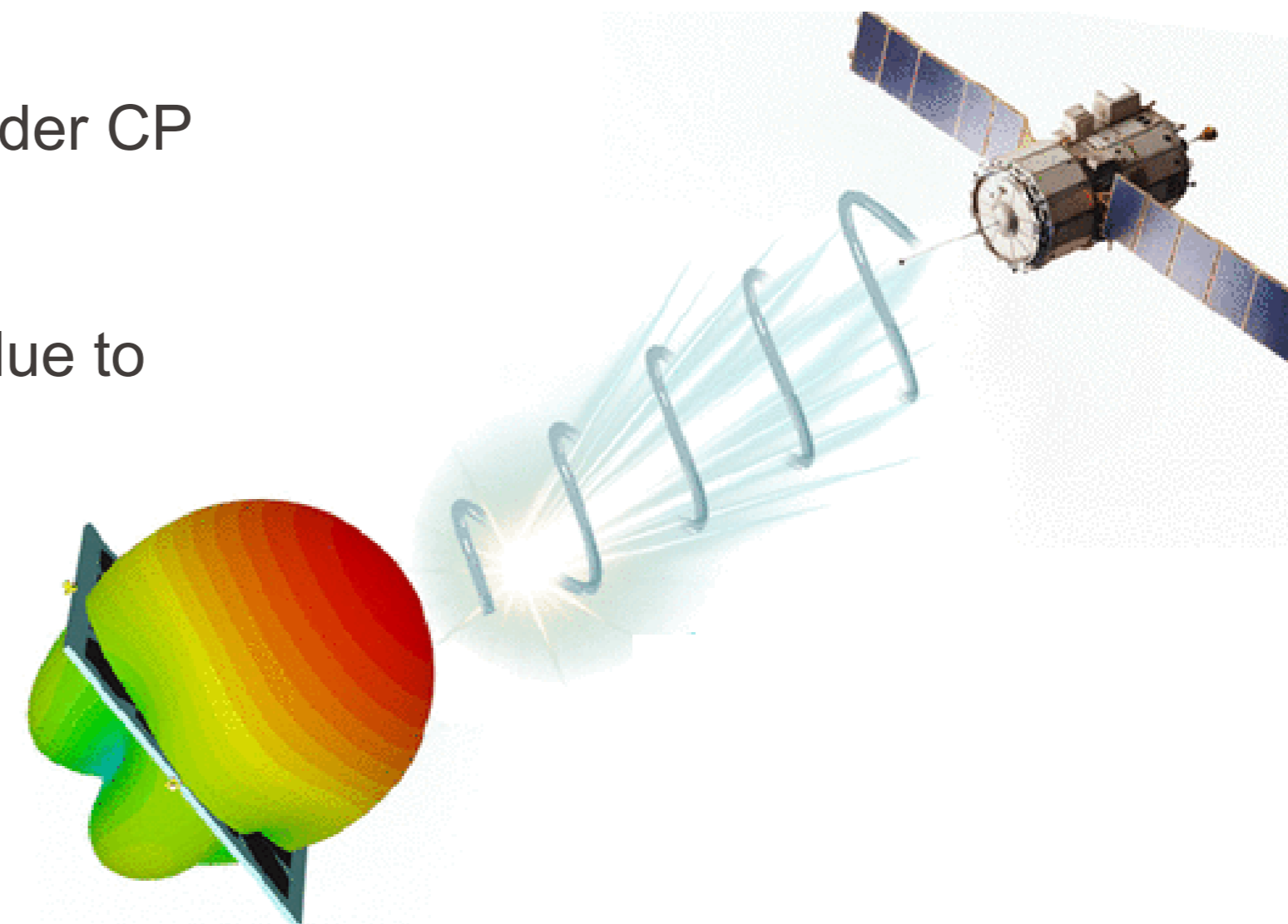
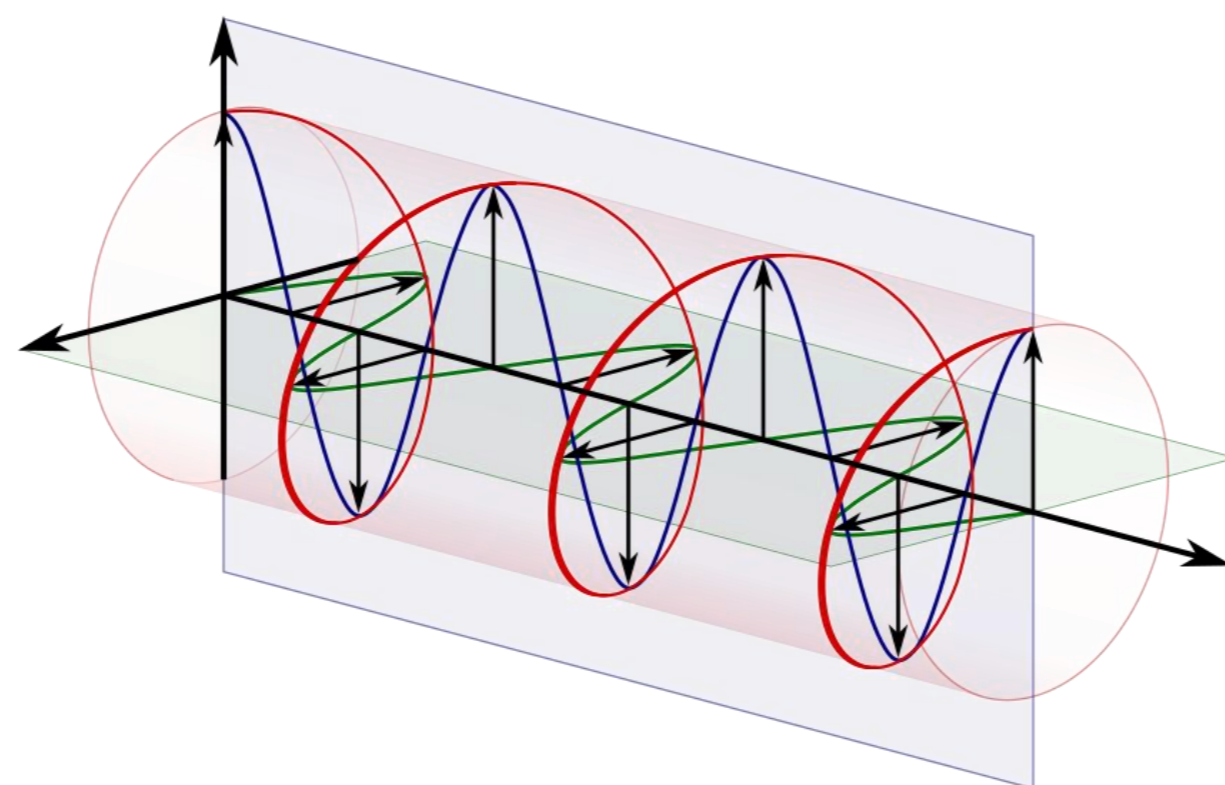
Circular Polarization

Circular polarization can be obtained if **two orthogonal modes** are excited with a **90° time-phase difference** between them. This can be accomplished by adjusting the physical dimensions of the patch and using either single, two, or multiple feeds.



Three main techniques:

- 1) Single feed with “nearly degenerate” eigenmodes (compact but small CP bandwidth).
- 2) Dual feed with a delay line or a 90° hybrid phase shifter (broader CP bandwidth but uses more space).
- 3) Synchronous subarray technique (produces high-quality CP due to cancellation effect, but requires even more space).



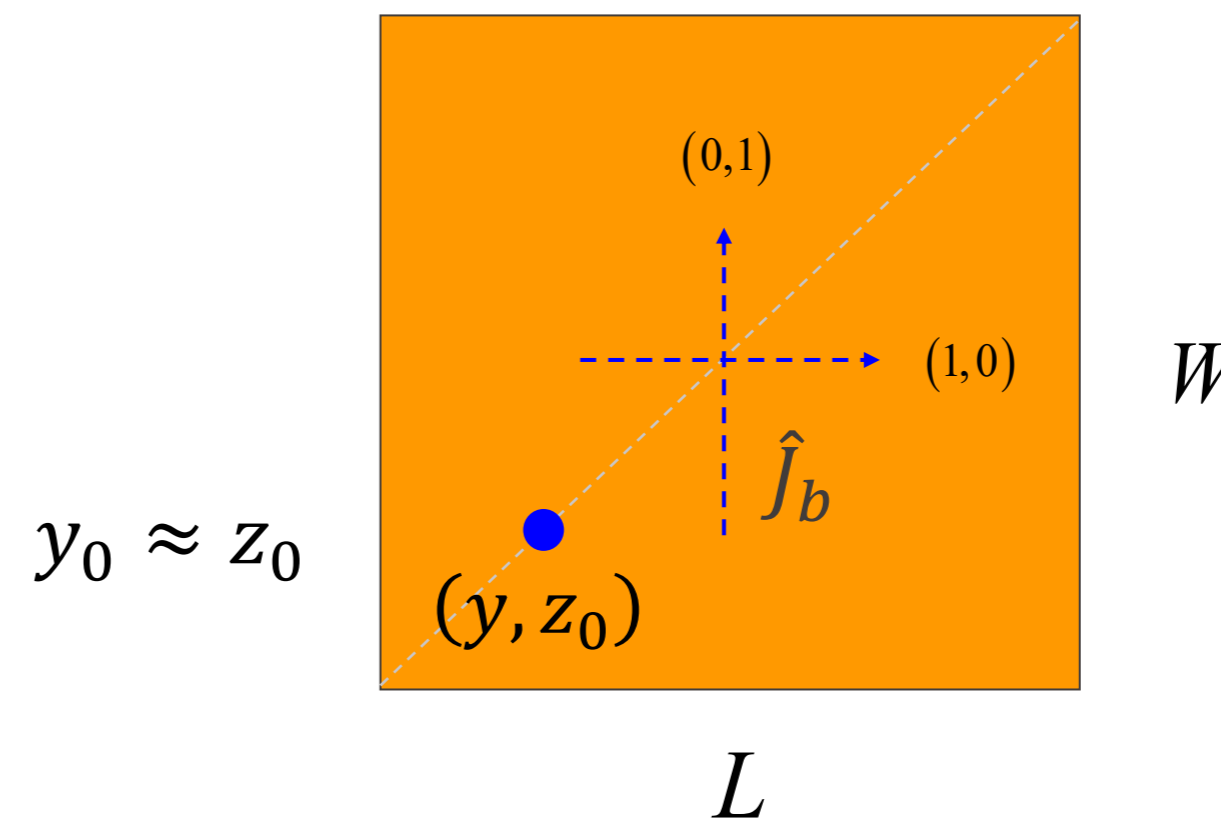
Circular Polarization

Single-Feed Structure

Basic principle: The two dominant modes (1,0) and (0,1) are excited with equal amplitude, but with a $\pm 45^\circ$ phase.

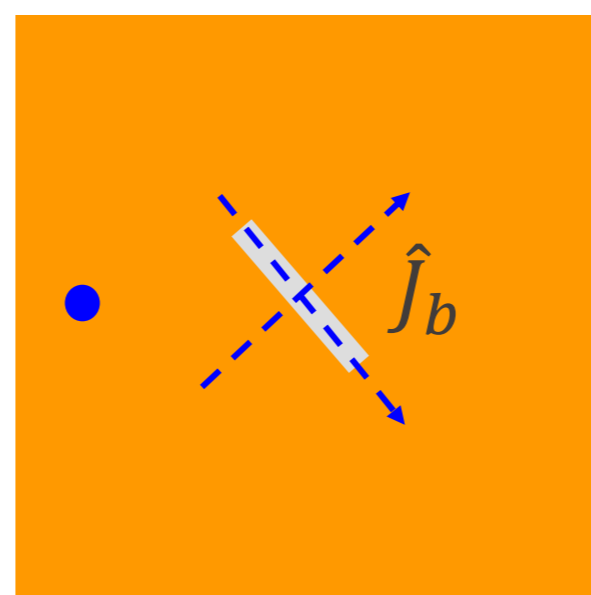
1. The feed is on the diagonal. The patch is nearly (but not exactly) square.

$$L \approx W$$



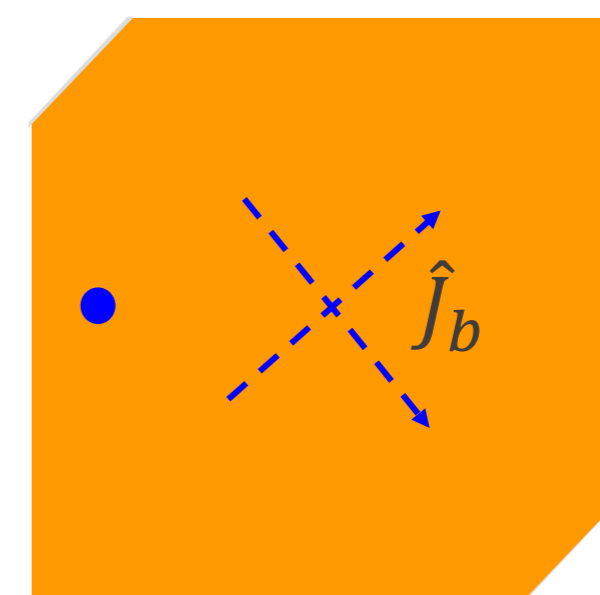
2. Using degenerate modes

Patch with slot



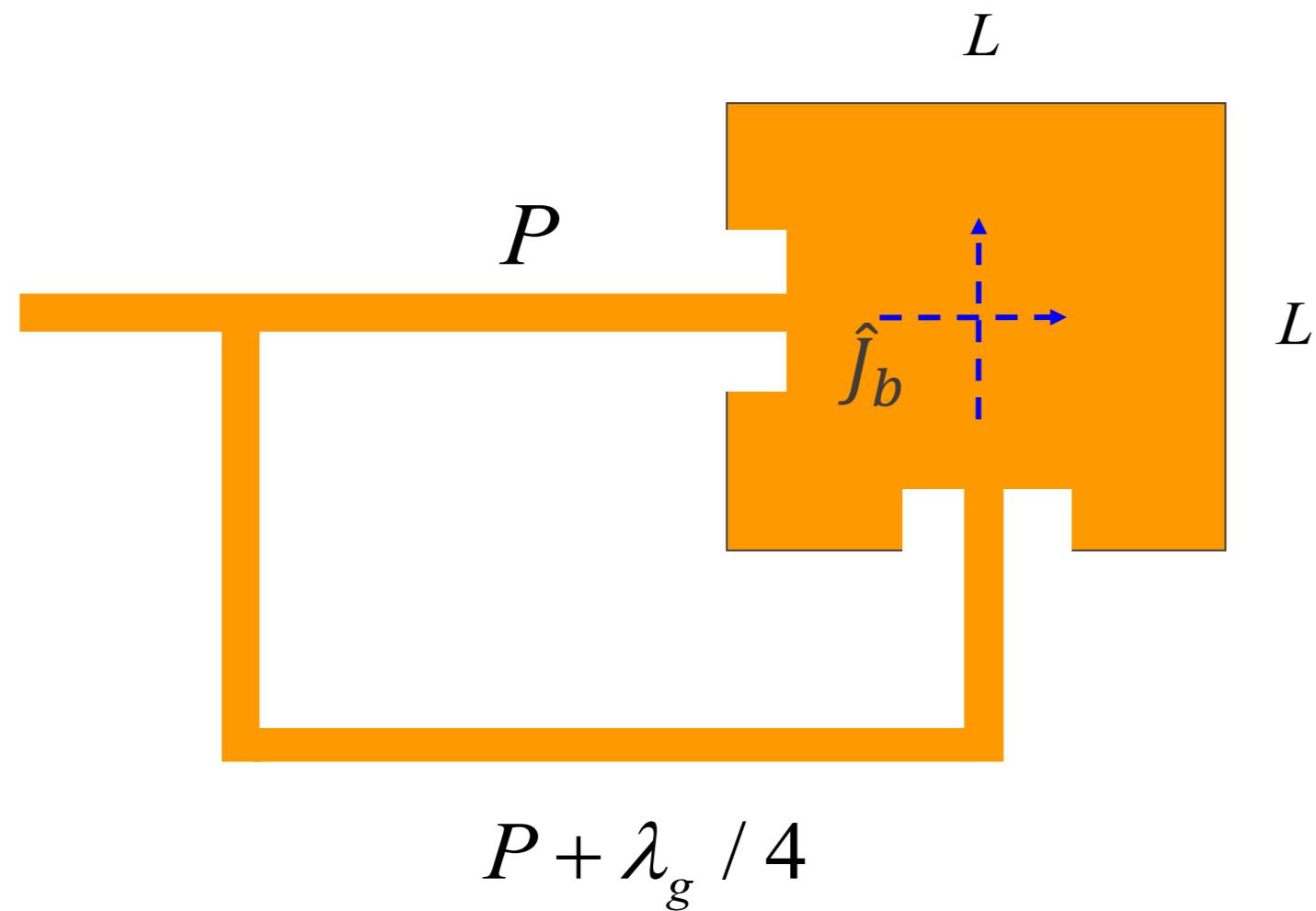
L

Patch with truncated corners



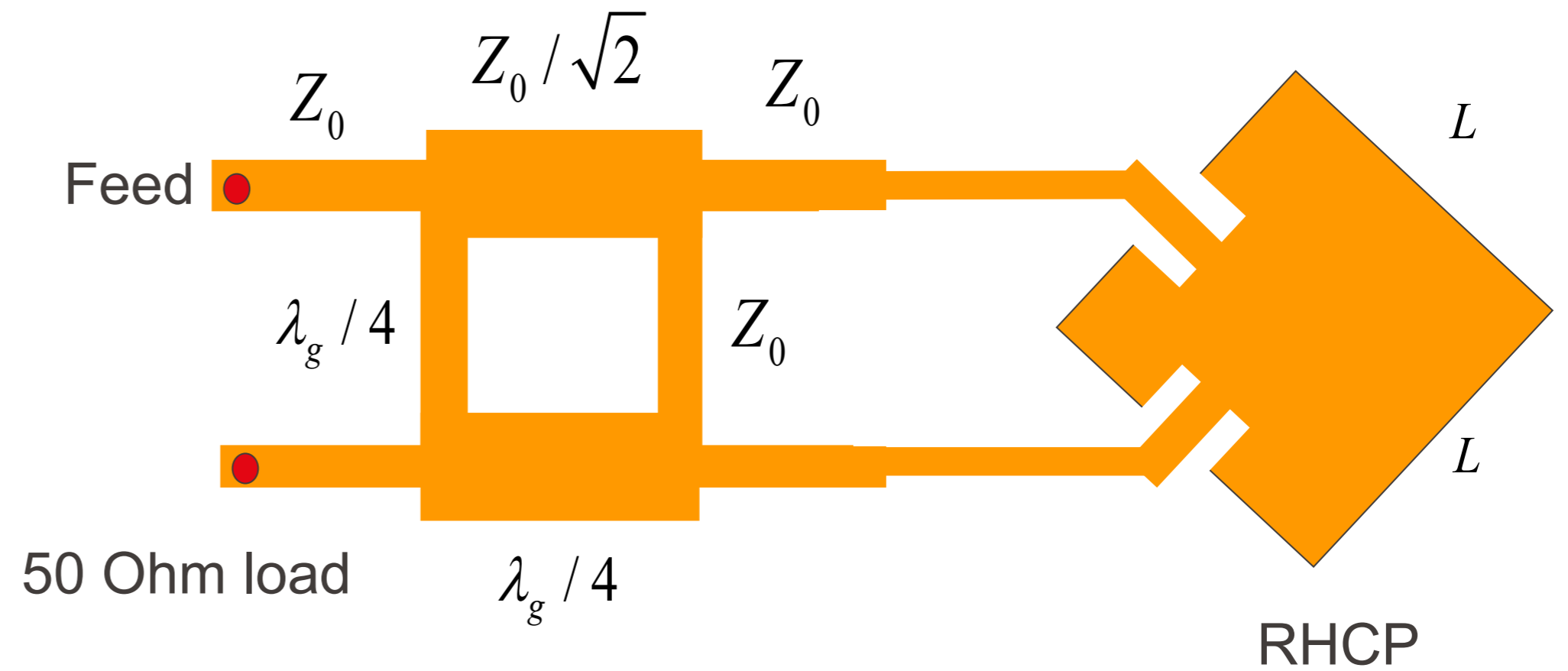
L

Phase shift realized with a delay line:



Antennas

Phase shift realized with 90° quadrature hybrid (branchline coupler)

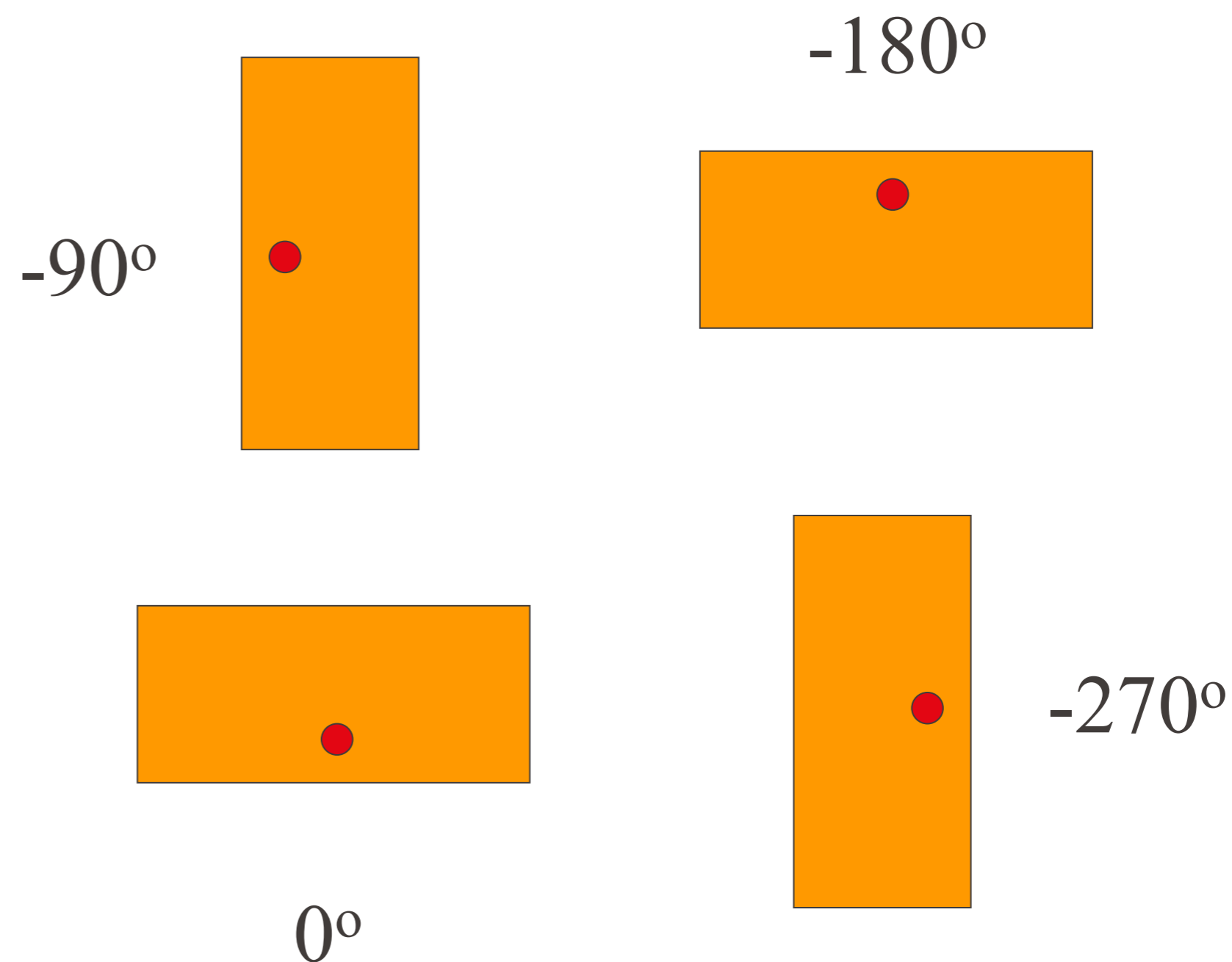


This gives us a higher bandwidth than the simple power divider, but requires a load resistor.

Multiple elements are rotated in space and fed with phase shifts.

Because of symmetry, radiation from higher-order modes (or probes) tends to be reduced, resulting in good cross-pol.

Antennas



Thank you!